A Tungsten Complex with a Bidentate, Hemilabile N-Heterocyclic Carbene Ligand, Facile Displacement of the Weakly Bound W−(C═C) Bond, and the Vulnerability of the NHC Ligand toward Catalyst Deactivation during Ketone Hydrogenation

Fan Wu,[†] Vladimir K. Dioumaev,[†] David J. Szalda,[†,‡] Jonathan Hanson,[†] and R. Morris Bullock*[,†,§]

Chemistry Department, Brookhaven National Laboratory, Upton, New York 11973-5000, and Chemical Sciences Division, Pacific Northwest National Laboratory, P.O. Box 999, K2-57, Richland, Washington 99352

Received July 12, 2007

The initial reaction observed between the N-heterocyclic carbene IMes (IMes = 1,3-bis(2,4,6-trimethylphenyl)imidazol-2-ylidene) and molybdenum and tungsten hydride complexes $CpM(CO)_2(PPh_3)H$ (M = Mo, W) is deprotonation of the metal hydride by IMes, giving $[(IMes)H]^+[CpM(CO)_2(PPh_3)]^-$. At longer reaction times and higher temperatures, the reaction of IMes with $CpM(CO)_2(PR_3)H$ (M = Mo, W; R = Me, Ph) produces $CpM(CO)_2(IMes)H$. Hydride transfer from $CpW(CO)_2(IMes)H$ to $Ph_3C^+B(C_6F_5)_4^-$ gives $CpW(CO)_2(IMes)^+B(C_6F_5)_4^-$, which was crystallographically characterized using X-ray radiation from a synchrotron. The IMes is bonded as a bidentate ligand, through the carbon of the carbene as well as forming a weak bond from the metal to a C═C bond of one mesityl ring. The weakly bound C═C ligand is hemilabile, being readily displaced by H_2, THF, ketones, or alcohols. Reaction of $CpW(CO)_2(IMes)^+$ with H_2 gives the dihydride complex $[CpW(CO)_2(IMes)(H)_2]^+$. Addition of Et_2CH-OH to $CpW(CO)_2(IMes)^+B(C_6F_5)_4^-$ gives the alcohol complex $[CpW(CO)_2(IMes)(Et_2CH-OH)]^+[B(C_6F_5)_4]^-$, which was characterized by crystallography and exhibits no evidence for hydrogen bonding of the bound OH group. Addition of H_2 to the ketone complex $[CpW(CO)_2(IMes)(Et_2C═O)]^+[B(C_6F_5)_4]^-$ produces an equilibrium with the dihydride $[CpW(CO)_2(IMes)(H)_2]^+$ ($K_{eq} = 1.1 \times 10^3$ at 25 °C). The tungsten ketone complex $[CpW(CO)_2(IMes)(Et_2C═O)]^+[B(C_6F_5)_4]^-$ serves as a modest catalyst for hydrogenation of $Et_2C═O$ to Et_2CH-OH in neat ketone solvent. Decomposition of the catalyst produces $[H(IMes)]^+B(C_6F_5)_4^-$, indicating that these catalysts with N-heterocyclic carbene ligands are vulnerable to decomposition by a reaction that produces a protonated imidazolium cation.

Introduction

Traditional homogeneous catalysts for ketone hydrogenation use Rh or Ru as the metal and proceed by mechanisms involving insertion of a ketone into a metal hydride bond.[1] Removing the mechanistic requirement for an insertion reaction opens the possibility of alternative mechanisms that may be feasible using a wider range of metals, including inexpensive alternatives to precious metals.[2] We found that phosphine-containing Mo and W complexes $[Cp(CO)_2(PR_3)M(O═CEt_2)]^+BAr'_4^-$ [R = Me, Ph, Cy; Ar′ = 3,5-bis(trifluoromethyl)phenyl] serve as catalyst precursors for the ionic hydrogenation of ketones.[3] Mechanistic studies show that these reactions proceed by an ionic hydrogenation mechanism,[2] in which proton transfer from a cationic metal dihydride to a ketone is followed by hydride transfer from a neutral metal hydride. The lifetime of the catalysts was limited by decomposition pathways that appear to be initiated by dissociation of a phosphine. A second generation of catalysts was designed to suppress phosphine dissociation by connecting the cyclopentadienyl and phosphine ligands through a two-carbon bridge,[4] and improved lifetimes and increased thermal stability were obtained.

N-Heterocyclic carbene (NHC) ligands[5] can offer significant advantages in comparison to phosphine ligands. Experimental studies[6,7] as well as computations[7,8] have shown that NHC

* Address correspondence to this author at PNNL. E-mail: morris.bullock@pnl.gov.

[†] Brookhaven National Laboratory.

[‡] Research Collaborator at Brookhaven National Laboratory. Permanent address: Department of Natural Sciences, Baruch College, New York, NY.

[§] Pacific Northwest National Laboratory.

(1) (a) Chaloner, P. A.; Esteruelas, M. A.; Joó, F.; Oro, L. A. *Homogeneous Hydrogenation*; Kluwer Academic Publishers: Boston, 1994. (b) Morris, R. H. Ruthenium and Osmium. In *Handbook of Homogeneous Hydrogenation*; de Vries, J. G., Elsevier, C. J., Eds.; Wiley-VCH: Weinheim, Germany, 2007; Chapter 3; Vol. 1.

(2) (a) Bullock, R. M. *Chem.−Eur. J.* **2004**, *10*, 2366−2374. (b) Bullock, R. M. Ionic Hydrogenations. In *The Handbook of Homogeneous Hydrogenations*; de Vries, J. G., Elsevier, C. J., Eds.; Wiley-VCH: Weinheim, Germany, 2007; Chapter 7, Vol. 1.

(3) (a) Bullock, R. M.; Voges, M. H. *J. Am. Chem. Soc.* **2000**, *122*, 12594−12595. (b) Voges, M. H.; Bullock, R. M. *J. Chem. Soc., Dalton Trans.* **2002**, 759−770.

(4) (a) Kimmich, B. F. M.; Fagan, P. J.; Hauptman, E.; Bullock, R. M. *Chem. Commun.* **2004**, 1014−1015. (b) Kimmich, B. F. M.; Fagan, P. J.; Hauptman, E.; Marshall, W. J.; Bullock, R. M. *Organometallics* **2005**, *24*, 6220−6229.

(5) (a) Bourissou, D.; Guerret, O.; Gabbaï, F. P.; Bertrand, G. *Chem. Rev.* **2000**, *100*, 39−91. (b) Herrmann, W. A.; Köcher, C. *Angew. Chem., Int. Ed. Engl.* **1997**, *36*, 2162−2187. (c) Herrmann, W. A. *Angew. Chem., Int. Ed.* **2002**, *41*, 1290−1309. (d) Arduengo, A. J., III. *Acc. Chem. Res.* **1999**, *32*, 913−921. Scott, N. M.; Nolan, S. P. *Eur. J. Inorg. Chem.* **2005**, 1815−1828. (e) Nolan, S. P., Ed. *N-Heterocyclic Carbenes in Synthesis*; Wiley-VCH: Weinheim, 2006.

(6) Huang, J.; Schanz, H.-J.; Stevens, E. D.; Nolan, S. P. *Organometallics* **1999**, *18*, 2370−2375.

(7) Dorta, R.; Stevens, E. D.; Scott, N. M.; Costabile, C.; Cavallo, L.; Hoff, C. D.; Nolan, S. P. *J. Am. Chem. Soc.* **2005**, *127*, 2485−2495.

10.1021/om700694e CCC: $37.00
Publication on Web 08/28/2007

ligands generally form stronger bonds to the metal than phosphines, thus reducing the dissociation of the ligand from the metal. NHC ligands, like phosphines, are normally intended to function as innocent spectator two-electron donors. NHC ligands can become bidentate ligands by undergoing ortho-metalation or cyclometalation[9−13] or dehydrogenation reactions.[14] Insertion reactions[15] and C−N cleavage[13,16] have also been observed in complexes with NHC ligands. These types of reactions alter the backbone of the NHC ligand by rupturing strong C−H or C−C bonds. In other cases, reversible weak coordination modes, such as agostic bonding or hydrogen bonding, have been observed for NHC ligands bearing aromatic ligands that are not protected by steric bulk.[10,17] We report synthetic, structural, and reactivity studies on a series of molybdenum and tungsten complexes with the widely used NHC ligand IMes (IMes = 1,3-bis(2,4,6-trimethylphenyl)imidazol-2-ylidene) and an evaluation of their use in the catalytic ionic hydrogenation of ketones.[18] We describe examples of cationic complexes where the IMes ligand functions as an overall four-electron donor, through the expected interaction of a bond to the carbene carbon and additionally through a weak interaction of the metal with a C=C bond of the mesityl ring. The NHC ligand is thus a bidentate hemilabile[19] ligand. Hemilabile ligands can be advantageous in catalysis, since the flexibility of multiple binding modes enables the ligand to temporarily protect a vacant coordination site. Our studies also resulted in the observation of cleavage of the NHC ligand during catalysis, resulting in protonated imidazolium cations. This exposes a vulnerability of these catalysts containing NHC ligands.

Results and Discussion

Synthesis and Characterization of $CpM(CO)_2(IMes)H$. Neutral molybdenum and tungsten complexes $CpM(CO)_2(IMes)H$ were synthesized from $CpM(CO)_2(PR_3)H$ (R = Me, Ph) by displacement of the phosphine ligand by the N-heterocyclic carbene ligand IMes. The reaction of IMes with $CpMo(CO)_2(PPh_3)H$ at room temperature in toluene results in the formation of a new complex that exhibits IR bands from CO ligands at 1778 and 1700 cm^{-1}, indicating a metal carbonyl anion. For comparison, the CO bands of $Li^+[CpMo(CO)_2(PMe_3)]^-$ appear at 1786 and 1646 cm^{-1} in THF.[20] In addition to resonances for the Cp and PPh_3 ligands, the ^1H NMR spectrum displays a singlet at δ 10.82 in C_6D_6 (δ 11.35 in CD_2Cl_2) assigned to the CH proton of the imidazolium cation. For comparison, the ^1H NMR spectrum of $[H(IMes)]^+Cl^-$ in CD_2Cl_2 exhibits a resonance at δ 11.27. These spectral features indicate that the complex is $[H(IMes)]^+[CpMo(CO)_2(PPh_3)]^-$, resulting from deprotonation of the metal hydride by IMes. Recrystallization of this complex gave an analytically pure sample. Analogous ionic complexes were observed spectroscopically in the reaction of IMes with $CpW(CO)_2(PPh_3)H$ and $CpMo(CO)_2(PMe_3)H$, but were not isolated in pure form.

The deprotonation of $CpMo(CO)_2(PPh_3)H$ and related metal hydrides by the NHC can be understood by considering the acidity of the metal hydride and the basicity of the NHC. Norton and co-workers determined the pK_a of $CpW(CO)_2(PMe_3)H$ to be 26.6 in CH_3CN.[21,22] The acidity of the Mo analogue was not determined, but Mo hydrides are more acidic than those of W; the pK_a of $CpMo(CO)_3H$ in CH_3CN is 13.9, versus 16.1 for $CpW(CO)_3H$.[21] A computational study predicted the pK_a values for a series of protonated NHC ligands in CH_3CN and DMSO solvents.[23] The pK_a found for an analogue of protonated IMes (with xylyl groups in the computational study rather than mesityl groups in IMes) was about 28.2 in CH_3CN and 16.8 in DMSO. This pK_a value in CH_3CN shows that deprotonation of metal hydrides such as $CpMo(CO)_2(PPh_3)H$ by NHCs should readily occur. NHC ligands with alkyl rather than aryl substituents were more basic, with computed pK_a values of their conjugate acids around 32−34 in CH_3CN and 21−24 in DMSO, in reasonable agreement with experimental values determined in DMSO[24] or aqueous solution.[25] Thus while some caution is needed in comparing relative acidities measured in different solvents (or extrapolated from one solvent to another), the specific values as well as the general trends support our experimental observations of initial deprotonation of metal hydrides by NHC ligands.

Displacement of a phosphine by an N-heterocyclic carbene ligand is commonly used as a synthetic procedure, but is generally applied to reactions where the other ligands on the metal are unreactive with the free NHC. Previous examples of

(8) Lee, M.-T.; Hu, C.-H. *Organometallics* **2004**, *23*, 976−983.
(9) (a) Hitchcock, P. B.; Lappert, M. F.; Pye, P. L.; Thomas, S. *J. Chem. Soc., Dalton Trans.* **1979**, 1929−1942. (b) Hitchcock, P. B.; Lappert, M. F.; Pye, P. L. *J. Chem. Soc., Chem. Commun.* **1977**, 196−198. (c) Huang, J.; Stevens, E. D.; Nolan, S. P. *Organometallics* **2000**, *19*, 1194−1197. (d) Trnka, T. M.; Morgan, J. P.; Sanford, M. S.; Wilhelm, T. E.; Scholl, M.; Choi, T.-L.; Ding, S.; Day, M. W.; Grubbs, R. H. *J. Am. Chem. Soc.* **2003**, *125*, 2546−2558. (e) Abdur-Rashid, K.; Fedorkiw, T.; Lough, A. J.; Morris, R. H. *Organometallics* **2004**, *23*, 86−94. (f) Dorta, R.; Stevens, E. D.; Nolan, S. P. *J. Am. Chem. Soc.* **2004**, *126*, 5054−5055. (g) Scott, N. M.; Dorta, R.; Stevens, E. D.; Correa, A.; Cavallo, L.; Nolan, S. P. *J. Am. Chem. Soc.* **2005**, *127*, 3516−3526. (h) Cariou, R.; Fischmeister, C.; Toupet, L.; Dixneuf, P. H. *Organometallics* **2006**, *25*, 2126−2128. (i) Burling, S.; Paine, B. M.; Nama, D.; Brown, V. S.; Mahon, M. F.; Prior, T. J.; Pregosin, P. S.; Whittlesey, M. K.; Williams, J. M. J. *J. Am. Chem. Soc.* **2007**, *129*, 1987−1995. (j) Ampt, K. A. M.; Burling, S.; Donald, S. M. A.; Douglas, S.; Duckett, S. B.; Macgregor, S. A.; Perutz, R. N.; Whittlesey, M. K. *J. Am. Chem. Soc.* **2006**, *128*, 7452−7453.
(10) Danopoulos, A. A.; Winston, S.; Hursthouse, M. B. *J. Chem. Soc., Dalton Trans.* **2002**, 3090−3091.
(11) Jazzar, R. F. R.; Macgregor, S. A.; Mahon, M. F.; Richards, S. P.; Whittlesey, M. K. *J. Am. Chem. Soc.* **2002**, *124*, 4944−4945.
(12) Burling, S.; Mahon, M. F.; Paine, B. M.; Whittlesey, M. K.; Williams, J. M. J. *Organometallics* **2004**, *23*, 4537−4539.
(13) Burling, S.; Mahon, M. F.; Powell, R. E.; Whittlesey, M. K.; Williams, J. M. J. *J. Am. Chem. Soc.* **2006**, *128*, 13702−13703.
(14) Prinz, M.; Grosche, M.; Herdtweck, E.; Herrmann, W. A. *Organometallics* **2000**, *19*, 1692−1694.
(15) (a) Danopoulos, A. A.; Tsoureas, N.; Green, J. C.; Hursthouse, M. B. *Chem. Commun.* **2003**, 756−757. (b) Becker, E.; Stingl, V.; Dazinger, G.; Puchberger, M.; Mereiter, K.; Kirchner, K. *J. Am. Chem. Soc.* **2006**, *128*, 6572−6573. (c) Galan, B. R.; Gembicky, M.; Dominiak, P. M.; Keister, J. B.; Diver, S. T. *J. Am. Chem. Soc.* **2005**, *127*, 15702−15703. (d) Fantasia, S.; Jacobsen, H.; Cavallo, L.; Nolan, S. P. *Organometallics* **2007**, *26*, 3286−3288. (e) Becker, E.; Stingl, V.; Dazinger, G.; Mereiter, K.; Kirchner, K. *Organometallics* **2007**, *26*, 1531−1535.
(16) Caddick, S.; Cloke, F. G. N.; Hitchcock, P. B.; Lewis, A. K. D. *Angew. Chem., Int. Ed.* **2004**, *43*, 5824−5827.
(17) Hitchcock, P. B.; Lappert, M. F.; Terreros, P. *J. Organomet. Chem.* **1982**, *239*, C26−C30.
(18) A preliminary account of these results was communicated: Dioumaev, V. K.; Szalda, D. J.; Hanson, J.; Franz, J. A.; Bullock, R. M. *Chem. Commun.* **2003**, 1670−1671.
(19) Slone, C. S.; Weinberger, D. A.; Mirkin, C. A. *Prog. Inorg. Chem.* **1999**, *48*, 233−350. Braunstein, P.; Naud, F. *Angew. Chem., Int. Ed.* **2001**, *40*, 680−699.
(20) Malisch, W.; Lankat, R.; Schmitzer, S.; Pikl, R.; Posset, U.; Kiefer, W. *Organometallics* **1995**, *14*, 5622−5627.
(21) Moore, E. J.; Sullivan, J. M.; Norton, J. R. *J. Am. Chem. Soc.* **1986**, *108*, 2257−2263.
(22) Kristjánsdóttir, S. S.; Norton, J. R. Acidity of Hydrido Transition Metal Complexes in Solution. In *Transition Metal Hydrides*; Dedieu, A., Ed.; VCH: New York, 1991 (Chapter 9); pp 309−359.
(23) Magill, A. M.; Cavell, K. J.; Yates, B. F. *J. Am. Chem. Soc.* **2004**, *126*, 8717−8724.
(24) (a) Kim, Y.-J.; Streitwieser, A. *J. Am. Chem. Soc.* **2002**, *124*, 5757−5761. (b) Alder, R. W.; Allen, P. R.; Williams, S. J. *J. Chem. Soc., Chem. Commun.* **1995**, 1267−1268.
(25) Amyes, T. L.; Diver, S. T.; Richard, J. P.; Rivas, F. M.; Toth, K. *J. Am. Chem. Soc.* **2004**, *126*, 4366−4374.

Scheme 1

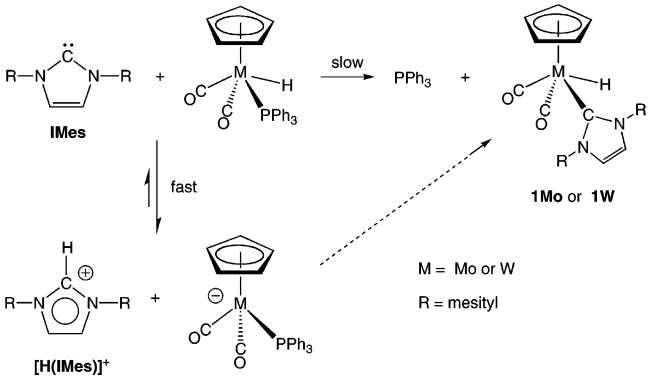

displacement of a phosphine by an NHC ligand on Ru[11,26] or Rh[27] hydride complexes involved metal hydrides that had two or more phosphines. Presumably the much lower acidity of such hydride complexes makes an initial deprotonation of the metal hydride by the NHC less favorable.

The rate of conversion of ionic $[H(IMes)]^+[CpM(CO)_2(PR_3)]^-$ to the neutral product $CpM(CO)_2(IMes)H$ (Scheme 1) is highly solvent-dependent. On a preparative scale, $CpMo(CO)_2(IMes)H$ was isolated in 86% yield after heating $CpMo(CO)_2(PPh_3)H$ and IMes at 95 °C in toluene for 3 h. In more polar solvents, however, the ionic complex is stabilized, and conversion of $[H(IMes)]^+[CpMo(CO)_2(PPh_3)]^-$ to $CpMo(CO)_2(IMes)H$ is much slower. In THF-d_8, 60% conversion was observed after 1 day at 95 °C. When $[H(IMes)]^+[CpMo(CO)_2(PPh_3)]^-$ was heated in CD_3CN for 7 days at 95 °C, only 5% conversion to $CpMo(CO)_2(IMes)H$ was detected. This remarkable solvent effect is attributed to the stabilization of the ionic species $[H(IMes)]^+[CpM(CO)_2(PR_3)]^-$ by polar solvents.

While the hydride complexes $CpM(CO)_2(IMes)H$ (for both M = Mo and W) can be purified by recrystallization to separate them from the PPh_3 released from $CpM(CO)_2(PPh_3)H$, use of $CpM(CO)_2(PMe_3)H$ as the starting material allows the volatile PMe_3 to be readily removed under vacuum. The entire reaction can be conveniently carried out under dynamic vacuum in the molten phase of neat reagents, $CpM(CO)_2(PMe_3)H$ and IMes, at 95−120 °C.

We suggest that the observed proton transfer reaction is an unproductive equilibrium and that $CpM(CO)_2(IMes)H$ forms as the product despite the intervention of this equilibrium. An alternate possibility is that $[H(IMes)]^+[CpM(CO)_2(PR_3)]^-$ is an intermediate on the pathway to formation of $CpM(CO)_2(IMes)H$. This mechanism would involve oxidative addition of the C−H bond of the imidazolium cation to the tungsten, presumably following dissociation of the PPh_3 ligand to generate a vacant site. Oxidative addition of imidazolium cations to metals has been observed in reactions of Ni, Pd, and Pt complexes,[28,29] as well as in studies of Rh and Ir complexes,[30] so there is substantial precedent for such reactivity of late metal complexes.

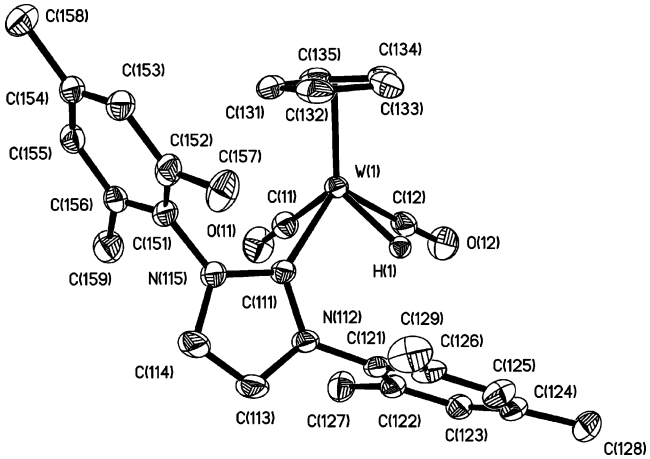

Figure 1. ORTEP diagram of complex $CpW(CO)_2(IMes)H$ (30% probability ellipsoids). H atoms are omitted except for the W*H*. Selected bond lengths (Å) and angles (deg): W(1)−C(11) 1.936(6), W(1)−C(12) 1.927(5), W(1)−C(111) 2.183(5), C(11)−W(1)−C(12) 77.7(2), C(11)−W(1)−C(111) 80.3(2), C(12)−W(1)−C(111) 109.68(19), N(112)−C(111)−W(1) 128.8(3), N(115)−C(111)−W(1) 129.3(3). Closest W···$C_{mesityl}$ nonbonding distances (Å): W(1)···C(121) 3.637(5), W(1)···C(151) 3.663(5).

On the other hand, oxidative addition pathways are less commonly observed for tungsten complexes of the type studied here (compared to Pd, Ir, etc.). We cannot rule out the direct oxidative addition pathway shown by the dotted arrow in Scheme 1.

The ^1H and ^{13}C chemical shifts of $CpW(CO)_2(IMes)H$ are indicative of the normal bonding mode of IMes through the N*C*N carbon, rather than through C-4 or C-5 of the imidazolium ring, denoted as "abnormal" by Crabtree.[31] In the $^{13}C\{^1H\}$ NMR spectrum at 27 °C, the CO ligands of $CpW(CO)_2(IMes)H$ appear as a slightly broadened singlet at δ 238, but at −100 °C the two CO ligands are inequivalent, appearing at δ 247.4 and 232.3. The four ortho-methyl groups of the IMes ligand appear as a singlet (12 H) at 27 °C in the ^1H NMR spectrum, but at −100 °C two separate singlets (6H each) are observed; a similar situation is found in the $^{13}C\{^1H\}$ NMR spectrum. An estimate of the OC−W−CO angle can be made from the relative areas of the two CO bands using the equation $\tan^2\theta = I_{asym}/I_{sym}$, where 2θ is the OC−M−CO angle and I_{asym} and I_{sym} are the relative integrated intensities of the asymmetric and symmetric CO bands.[32] The IR spectrum of $CpW(CO)_2(IMes)H$ in CD_2Cl_2 exhibits ν_{sym}(CO) at 1906 cm^{-1} and ν_{asym}(CO) at 1810 cm^{-1}. The experimentally measured value of $I_{asym}/I_{sym} = 0.95$ leads to a predicted OC−M−CO angle of 89°, indicating that the two CO ligands are cis to each other. This configuration renders the metal a chiral center, in agreement with the low-temperature NMR data.

Molecular Structures of $CpW(CO)_2(IMes)H$ and $CpMo(CO)_2(IMes)H$ by Single-Crystal X-ray Diffraction. The structures of $CpW(CO)_2(IMes)H$ and $CpMo(CO)_2(IMes)H$ were determined by X-ray diffraction and are unremarkable four-legged piano stools (Figures 1 and 2). The carbonyls are cis, as surmised by the NMR and IR data. The IMes ligand is coordinated symmetrically, as indicated by very similar N−C−W angles.

(26) Giunta, D.; Hölscher, M.; Lehmann, C. W.; Mynott, R.; Wirtz, C.; Leitner, W. *Adv. Synth. Catal.* **2003**, *345*, 1139−1145.
(27) Douglas, S.; Lowe, J. P.; Mahon, M. F.; Warren, J. E.; Whittlesey, M. K. *J. Organomet. Chem.* **2005**, *690*, 5027−5035.
(28) (a) McGuinness, D. S.; Cavell, K. J.; Yates, B. F.; Skelton, B. W.; White, A. H. *J. Am. Chem. Soc.* **2001**, *123*, 8317−8328. (b) Clement, N. D.; Cavell, K. J.; Jones, C.; Elsevier, C. J. *Angew. Chem., Int. Ed.* **2004**, *43*, 1277−1279.
(29) Gründemann, S.; Albrecht, M.; Kovacevic, A.; Faller, J. W.; Crabtree, R. H. *J. Chem. Soc., Dalton Trans.* **2002**, 2163−2167.
(30) (a) Viciano, M.; Mas-Marzá, E.; Poyatos, M.; Sanaú, M.; Crabtree, R. H.; Peris, E. *Angew. Chem., Int. Ed.* **2005**, *44*, 444−447. (b) Viciano, M.; Poyatos, M.; Sanau, M.; Peris, E.; Rossin, A.; Ujaque, G.; Lledos, A. *Organometallics* **2006**, *25*, 1120−1134.
(31) Gründemann, S.; Kovacevic, A.; Albrecht, M.; Faller, J. W.; Crabtree, R. H. *J. Am. Chem. Soc.* **2002**, *124*, 10473−10481.
(32) (a) King, R. B.; Riemann, R. H. *Inorg. Chem.* **1976**, *15*, 179−183. Brown, T. L.; Darensbourg, D. J. *Inorg. Chem.* **1967**, *6*, 971−977. (b) Beck, W.; Melnikoff, A.; Stahl, R. *Angew. Chem., Int. Ed. Engl.* **1967**, *4*, 692−693.

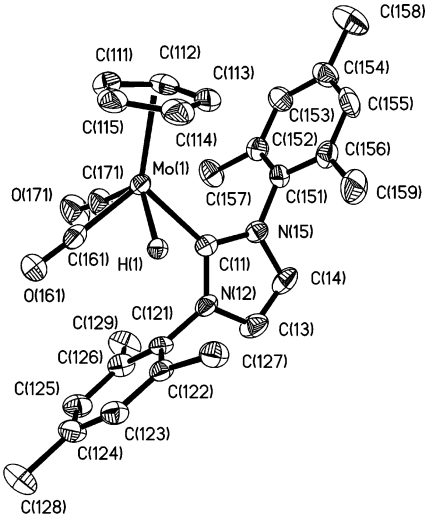

Figure 2. ORTEP diagram of complex $CpMo(CO)_2(IMes)H$ (30% probability ellipsoids). H atoms are omitted except for the Mo*H*. Selected bond lengths (Å) and angles (deg): Mo1−C161 1.948(11), Mo1−C171 1.955(12), Mo1−C11 2.187(8), Mo2−C211 1.917(10), Mo2−C271 1.935(11), Mo2−C21 2.171(8), C161−Mo1−C171 78.7(4), C161−Mo1−C11 104.9(3), C171−Mo1−C11 83.2(4), N12−C11−Mo1 128.6(6), N15−C11−Mo1 128.7(6), C211−Mo2−C271 80.0(4), C211−Mo2−C21 104.9(4), C271−Mo2−C21 82.5(4), N22−C21−Mo2 129.1(6), N25−C21−Mo2 128.5(6). Closest Mo···$C_{mesityl}$ nonbonding distances (Å): Mo1−C121 3.638(10), Mo1−C151 3.699(10).

Hydride Transfer from $CpM(CO)_2(IMes)H$ to $Ph_3C^+B(C_6F_5)_4^-$ to Give $CpM(CO)_2(IMes)^+B(C_6F_5)_4^-$. Hydride transfer from $CpM(CO)_2(IMes)H$ to $Ph_3C^+B(C_6F_5)_4^-$ gives cationic complexes $CpM(CO)_2(IMes)^+B(C_6F_5)_4^-$ (abbreviated as **Mo** or **W**) (eq 1). The reaction is complete within minutes at 25 °C,

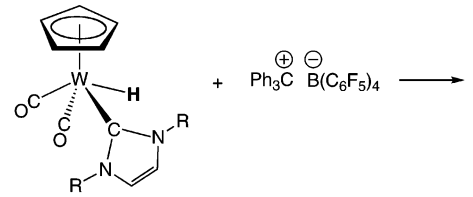

(1)

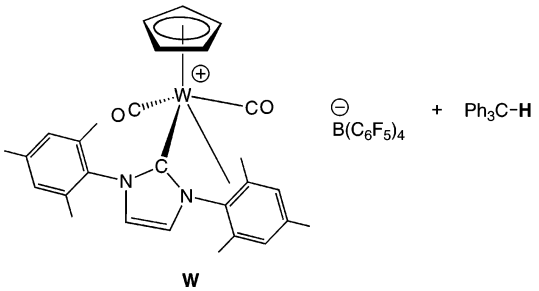

W

and the analytically pure product precipitates from toluene in high yield. IR bands for the CO ligands appear at much higher frequencies than those for the neutral hydrides. Bands for **Mo** (Nujol) appear at 1999 and 1905 cm^{-1}, while those for **W** appear at 1980 and 1890 cm^{-1}. Spectroscopic characterization of **W** is complicated by its reactivity and solubility characteristics, as it is insoluble in hexane or toluene, and reacts with more polar solvents. Prompt decomposition to unidentified products occurs when **W** is dissolved in CD_2Cl_2. Solutions of **W** in CF_3Ph are stable for longer times (roughly 10% decomposition in 22 h),

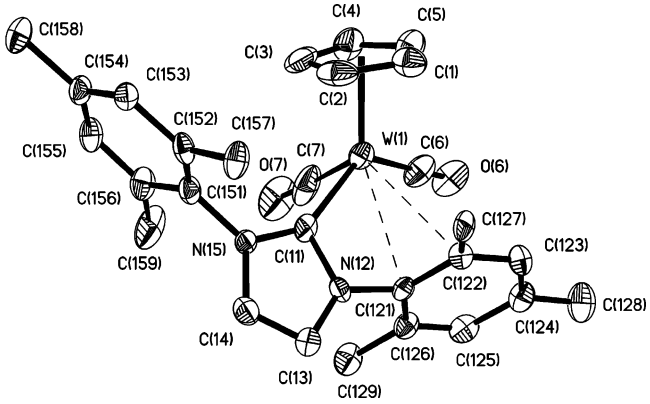

Figure 3. ORTEP diagram of the cation of $CpW(CO)_2(IMes)^+$-$B(C_6F_5)_4^-$ (**W**) (30% probability ellipsoids). H atoms are omitted. Selected bond lengths (Å) and angles (deg): W(1)−C(6) 1.928(15), W(1)−C(7) 1.934(19), W(1)−C(11) 2.188(12), W(1)−C(121) 2.901(13), W(1)−C(122) 3.072(13), C(6)−W(1)−C(7) 77.9(6), C(6)−W(1)−C(11) 129.5(5), C(7)−W(1)−C(11) 84.1(5), N(12)−C(11)−W(1) 113.9(8), N(15)−C(11)−W(1) 146.6(8).

which allows for ^1H NMR but not ^{13}C NMR characterization. Adducts are cleanly formed with coordinating solvents such as THF or ketones (*vide infra*).

Molecular Structure of $CpW(CO)_2(IMes)^+$. The lack of suitable solvents frustrated attempts to obtain single crystals of **W** suitable for conventional X-ray diffraction. However, use of high-intensity X-ray radiation at the National Synchrotron Light Source enabled a structural determination using the very small crystals (0.010 × 0.050 × 0.100 mm for **W**) obtained by slow diffusion of reactants in toluene. While the formula, $CpW(CO)_2(IMes)^+$, appears to indicate a 16-electron configuration at W, the crystal structure (Figure 3) reveals that a C═C bond of one of the mesityls forms a weak but distinct interaction to the metal: W(1)−C(121) 2.901(13) Å and W(1)−C(122) 3.072(13) Å.

These bonds are much longer than those found in complexes containing an η^2-arene ligand that is not chelated; M−(C═C) distances in η^2-arene complexes are typically 2.1−2.2 Å.[33] For complexes containing η^2-arenes constrained to the metal through chelation (as is the case in **W**) M−C lengths are often significantly longer, with distances as long as 2.5−2.8 Å being found in Mo and W complexes.[34]

The p-orbitals of the C═C point directly at the metal in **W**, as expected for this type of bonding interaction. (See Figure S1 of the Supporting Information.) In $CpW(CO)_2(IMes)H$, where there is no interaction of the C═C bonds to W, the N−C−W angles are nearly equivalent (128.8(3)° and 129(3)°; see Figure S2a of the Supporting Information). In contrast, distortions of the IMes ligand in **W** (Figure S2b of the Supporting Informa-

(33) (a) Winemiller, M. D.; Kelsch, B. A.; Sabat, M.; Harman, W. D. *Organometallics* **1997**, *16*, 3672−3678. (b) Chin, R. M.; Dong, L.; Duckett, S. B.; Partridge, M. G.; Jones, W. D.; Perutz, R. N. *J. Am. Chem. Soc.* **1993**, *115*, 7685−7695. (c) Tagge, C. D.; Bergman, R. G. *J. Am. Chem. Soc.* **1996**, *118*, 6908−6915. (d) Reinartz, S.; White, P. S.; Brookhart, M.; Templeton, J. L. *J. Am. Chem. Soc.* **2001**, *123*, 12724−12725.

(34) (a) Cobbledick, R. E.; Dowdell, L. R. J.; Einstein, F. W. B.; Hoyano, J. K.; Peterson, L. K. *Can. J. Chem.* **1979**, *57*, 2285−2291. (b) Jeffery, J. C.; Moore, I.; Razay, H.; Stone, F. G. A. *J. Chem. Soc., Chem. Commun.* **1981**, 1255−1258. (c) Curtis, M. D.; Messerle, L.; D'Errico, J. J.; Solis, H. E.; Barcelo, I. D.; Butler, W. M. *J. Am. Chem. Soc.* **1987**, *109*, 3603−3616. (d) Shiu, K.-B.; Chou, C.-C.; Wang, S.-L.; Wei, S.-C. *Organometallics* **1990**, *9*, 286−288. (e) Howard, J. A. K.; Jeffery, J. C.; Li, S.; Stone, F. G. A. *J. Chem. Soc., Dalton Trans.* **1992**, 627−634. (f) Shiu, K.-B.; Yeh, L.-Y.; Peng, S.-M.; Cheng, M.-C. *J. Organomet. Chem.* **1993**, *460*, 203−211. (g) Cheng, T.-Y.; Szalda, D. J.; Bullock, R. M. *J. Chem. Soc., Chem. Commun.* **1999**, 1629−1630.

tion) provide further indications of the bonding interaction: the N(12)−C(11)−W(1) angle is compressed to 113.9(8)°, and the N(15)−C(11)−W(1) angle is expanded to 146.6(8)°.

The electronic unsaturation in **W** results in distortion of the IMes ligand and bending of the mesityl substituent *toward* the metal for coordination. In contrast, other reported examples of electronic unsaturation in metal complexes with IMes ligands exhibit tilt of the mesityl groups *away* from the metal. Thus computations[35] on ruthenium complexes involved in the olefin metathesis catalysts developed by Grubbs and co-workers[36] indicate that the 14-electron species $(NHC)Cl_2Ru{=}C(H)Ph$ (formed by loss of PCy_3 from $(NHC)(PCy_3)Cl_2Ru{=}C(H)Ph$) has a characteristic tilt of mesityl groups *away* from the metal and alkylidene ligand to release steric pressure.

The methyl group of the interacting C═C fragment in **W** is bent out of the plane of the mesityl ring by 13.4° and away from the metal, in accord with the change in hybridization. As previously reported,[18] DFT computations also provide support for the bonding of the C═C bond of the mesityl ring to the metal for both Mo and W. The methyl substituent bonded to the C═C is displaced out of plane of the mesityl ring in the computed structures (8.2° for W and 7.2° for Mo), providing convincing evidence of bonding.

The solid-state structure of **Mo** was also determined from synchrotron data. It appears to be similar to that of **W**, but with shorter distances from the metal to the coordinated C═C (2.77-(3) and 3.02(3) Å). Unfortunately, the quality of the structural determination for **Mo** is marginal, so detailed structural comparisons are not warranted. Further information on the structure determination is provided in the Supporting Information.

Synthesis and Characterization of the Dihydride Complex $[CpW(CO)_2(IMes)(H)_2]^+[B(C_6F_5)_4]^-$. Reaction of H_2 with a suspension of **W** in toluene produces the dihydride complex $[CpW(CO)_2(IMes)(H)_2]^+[B(C_6F_5)_4]^-$ (**WH_2**) (eq 2). The carbonyl IR bands of **WH_2** appear at 2065 and 2006 cm^{-1} in C_6D_6 solution, with the higher frequency compared to **W** reflecting the higher oxidation state of **WH_2**. At 27 °C, a singlet is

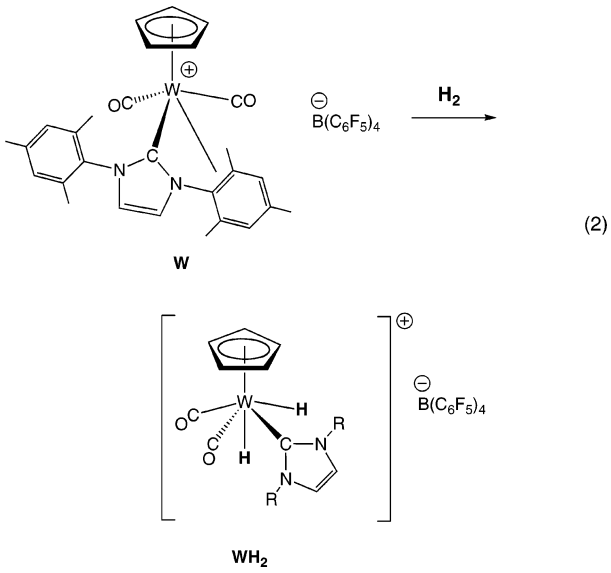

(2)

observed for the two hydrides at δ −0.72 in THF-d_8 solvent. This resonance broadens at lower temperatures, with $\nu_{1/2} \approx 138$ Hz at −18 °C. At −39 °C the resonance is nearly coalesced into the baseline ($\nu_{1/2} \approx 900$ Hz), and at −60 °C separate broad resonances ($\nu_{1/2} \approx 230$ Hz) are observed. Further sharpening of the inequivalent hydride resonances occur as the temperature is lowered, and at −100 °C two distinct resonances appear at δ 1.19 and −2.97. In the ^{13}C NMR spectrum at −100 °C, the two CO ligands are inequivalent (δ 205.2 and 203.1), as are the ortho-methyl groups on the mesityl fragment. These features indicate a lack of symmetry in the dihydride. The activation parameters of the fluxional process were determined by line shape analysis of the hydride resonances ($\Delta H^{\ddagger} = 9.3 \pm 0.3$ kcal mol^{-1} and $\Delta S^{\ddagger} = -2 \pm 1$ cal mol^{-1} K^{-1}, measured over the range −100 to 27 °C). The low entropy of activation is indicative of an intramolecular mechanism, but these data are insufficient to deduce the exact nature of the process. Thus, the enthalpy barrier value is consistent with several plausible dynamic processes, such as a hindered rotation of the bulky IMes ligand, a turnstile rotation of the $W(CO)(H)_2$ or $W(CO)_2H$ tripods, or even more elaborate mechanisms involving transient formation of dihydrogen complexes.[37] A cis-dicarbonyl configuration of **WH_2** is assigned on the basis of the relative intensity of the two carbonyl IR bands ($I_{asym}/I_{sym} = 1.1$; predicted OC−W−CO angle 93°) The structure suggested in eq 2 is consistent with the data that require inequivalent hydrides and cis carbonyls. This geometry, with one hydride "trans" to the Cp ligand, is analogous to that determined in the crystal structure of $[CpW(CO)_2(PMe_3)(H)_2]^+[OTf]^-$,[38] but other geometries cannot be ruled out on the basis of the spectral data.

Formation of 18e⁻ Adducts of $[CpM(CO)_2(IMes)]^+[B(C_6F_5)_4]^-$ with THF, $Et_2C{=}O$, and $Et_2CH{-}OH$. The weakly bound C═C ligand in $[CpM(CO)_2(IMes)]^+$ is readily displaced by oxygen donor ligands (THF, ketones, alcohols) to form the adducts $[CpM(CO)_2(IMes)(THF)]^+[B(C_6F_5)_4]^-$ (**Mo-(THF)** or **W(THF)**), $[CpM(CO)_2(IMes)(Et_2C{=}O)]^+[B(C_6F_5)_4]^-$ (**$Mo(Et_2C{=}O)$** or **$W(Et_2C{=}O)$**, and $([CpW(CO)_2(IMes)(Et_2CH{-}OH)]^+[B(C_6F_5)_4]^-$ (**$W(Et_2CHOH)$**) (eq 3). The metal carbonyl IR ν(CO) bands indicate adduct formation: 1977 and 1882 cm^{-1} for $[CpM(CO)_2(IMes)(THF\text{-}d_8)]^+[B(C_6F_5)_4]^-$, **Mo-(THF-*$d_8$*)**, and 1962 and 1859 cm^{-1} for **W(THF-*d_8*)**, indicating more electron density on the metal than in **Mo** or **W**, but less than in $CpM(CO)_2(IMes)H$ (1918 and 1843 cm^{-1} for $CpMo(CO)_2(IMes)H$ in THF-d_8; 1913 and 1822 cm^{-1} for $CpW(CO)_2(IMes)H$). The relative intensities of the CO bands are consistent with cis orientation of the carbonyls.

The ketone complex $[CpW(CO)_2(IMes)(Et_2C{=}O)]^+[B(C_6F_5)_4]^-$ (**$W(Et_2C{=}O)$**) is reasonably stable in solution but leaches ketone upon attempted recrystallization or washing with hydrocarbon solvents. Broadened resonances are observed in the ^1H NMR spectrum in C_6D_6 for the CH_2 and CH_3 groups of the ketone in $[CpW(CO)_2(IMes)(Et_2C{=}O)]^+[B(C_6F_5)_4]^-$, indicative of exchange of the ketone on and off the metal.

When Et_2CHOH is added to a suspension of **W** in benzene, a purple solution is formed. After 2 days, purple crystals of alcohol complex **$W(Et_2CHOH)$** are deposited (eq 3). In the IR spectrum (KBr), the ν(O−H) stretch is observed as a weak, broad band at 3420 cm^{-1}. The crystals were too small (0.050 × 0.050 × 0.005 mm) for a structure determination by conventional X-ray crystallography, so the structure was determined by single-crystal X-ray diffraction using the high-intensity X-ray radiation at the National Synchrotron Light

(35) Cavallo, L. *J. Am. Chem. Soc.* **2002**, *124*, 8965−8973.

(36) (a) Sanford, M. S.; Ulman, M.; Grubbs, R. H. *J. Am. Chem. Soc.* **2001**, *123*, 749−750. (b) Sanford, M. S.; Love, J. A.; Grubbs, R. H. *J. Am. Chem. Soc.* **2001**, *123*, 6543−6554.

(37) Ryan, O. B.; Tilset, M.; Parker, V. D. *J. Am. Chem. Soc.* **1990**, *112*, 2618−2626.

(38) Bullock, R. M.; Song, J.-S.; Szalda, D. J. *Organometallics* **1996**, *15*, 2504−2516.

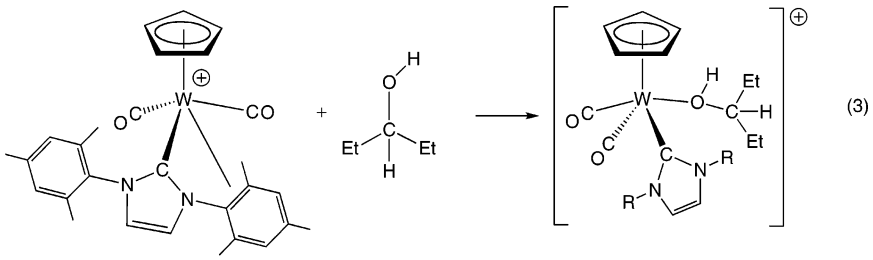

W **W(Et$_2$CHOH)**

(3)

Source. As shown in Figure 4, the alcohol ligand is cis to the IMes ligand. The W−O bond length of 2.250(7) Å is longer than the W−O bond length of 2.176(8) Å found in $[Cp(CO)_3W(HO^iPr)]^+OTf^-$.[39] In the ^{1}H NMR spectrum of **W(Et$_2$CHOH)** in C_6D_6, the resonance for the OH of the bound alcohol appears at δ 0.62. The OH resonance for the free alcohol (0.037 M in C_6D_6) appears at δ 0.67, indicating that coordination of the alcohol to the metal results in a very small perturbation of its chemical shift. We interpret this to indicate that there is little or no hydrogen bonding of the bound alcohol to any proton acceptor sites. We find no evidence for significant hydrogen bonding of the OH of the bound alcohol in the solid state of **W(Et$_2$CHOH).** The shortest O···F separation was 4.355 Å [from O(3) to F(85)], which is much too long of a distance to be considered for a hydrogen-bonding interaction. In contrast, most previously reported alcohol ligands engage in hydrogen bonding, as indicted by structural studies, as well as significant downfield shifts in the ^{1}H NMR spectrum of the bound OH peak. The crystal structure of $[Cp(CO)_3W(HO^iPr)]^+OTf^-$ [39] shows that the OH ligand is strongly hydrogen bonded to an oxygen of the triflate anion in the solid state, as evidenced by a short O···O distance of 2.63(1) Å. Evidence that the O−H···O hydrogen bonding persists in solution comes from the chemical shift of δ 7.34 of the OH of $[Cp(CO)_3W(HO^iPr)]^+OTf^-$ in the ^{1}H NMR spectrum in CD_2Cl_2 solution, with the large shift downfield compared to the free alcohol being indicative of hydrogen bonding. Beck and co-workers reported the crystal structure of $[Cp(CO)(PPh_3)Ru(EtOH)]^+BF_4^-$, which had O−H···F hydrogen bonding of the alcohol to the BF_4^- ligand and an O···F distance of 2.66 Å.[40] Spectroscopic evidence provided strong evidence of hydrogen bonding of the methanol ligand to the ClO_4^- anion in the rhenium complex $[ReH(CO)(NO)(PPh_3)_2(MeOH)]^+ClO_4^-$ reported by Grundy and Robertson.[41] Bochmann and co-workers showed[42] from a crystal structure that Et_2O forms a hydrogen bond to the bound isopropyl alcohol ligand in $[Cp_2Zr(O^iPr)(HO^iPr)]^+\cdot OEt_2$. In contrast, Gladysz and co-workers concluded that their spectroscopic data did not provide strong evidence for hydrogen bonding in the rhenium alcohol complexes $[CpRe(NO)(PPh_3)(ROH)]^+BF_4^-$.[43]

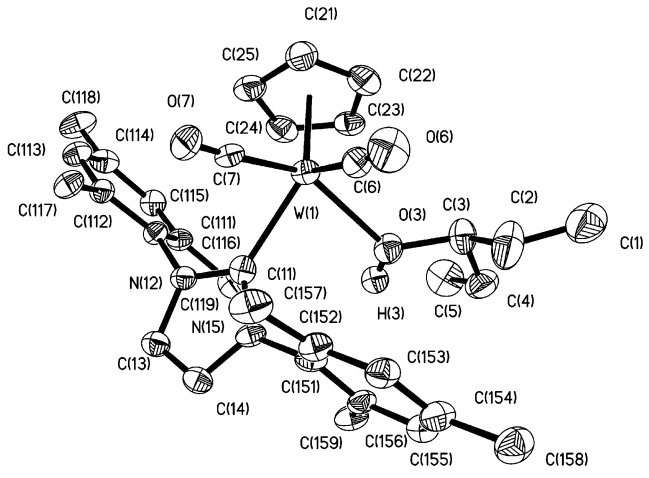

Figure 4. ORTEP of $[CpW(CO)_2(IMes)(Et_2CH-OH)]^+$ (30% probability ellipsoids). H atoms are omitted except for the O*H*. Selected bond lengths (Å) and angles (deg): W(1)−C(6) 1.945(14), W(1)−C(7) 1.966(12), W(1)−O(3) 2.250(7), C(6)−W(1)−C(7) 73.3(5), C(6)−W(1)−C(11) 111.9(4), C(7)−W(1)−C(11) 77.3(4).

Equilibria for Displacement of the Ketone or THF Ligand by H$_2$. Addition of $Et_2C{=}O$ to the tungsten cation **W** led to the immediate formation of the ketone complex $[CpW(CO)_2(IMes)(Et_2C{=}O)]^+[B(C_6F_5)_4]^-$ (**W(Et$_2$C=O)**; 0.047 M). When H_2 (4 atm) was added to this NMR tube, a ^{1}H NMR spectrum recorded at 0 °C showed that 58% of the tungsten complex had been converted to the dihydride complex **WH$_2$** (eq 4). The concentration of H_2 dissolved in solution was 9 mM; the integration of H_2 was corrected for the fact that 25% of the H_2 is para-H_2, which is NMR-silent. The equilibrium constant determined under these conditions was $K_{eq} = 1.4 \times 10^3$. The NMR tube was warmed to 25 °C, and the K_{eq} determined at

The adduct complexes readily convert into each other when two oxygen donors are present simultaneously. Thus, ^{1}H NMR signals of the THF complex **W(THF)** and ketone complex **W(Et$_2$C=O)** are broad in C_6D_6 but are sharp in neat THF or ketone. This behavior is consistent with a facile dissociation of the oxygen donor ligand and suppression of such dissociation by a large excess of ligand.

The $^{13}C\{^1H\}$ NMR spectrum of **W(THF-*d*$_8$)** in THF-d_8 at −40 °C indicates inequivalent CO ligands (δ 247.1, 246.2). In its cis configuration the metal is chiral and the two CO ligands are expected to be inequivalent. Inequivalent resonances for the CH=CH vinyl carbons (δ 128.4, 126.6) are observed in the $^{13}C\{^1H\}$ NMR. In addition, the two sides of the IMes ligand are inequivalent, exhibiting four separate resonances for the ortho-CH_3 groups on the mesityl rings in both the ^{1}H NMR spectrum at −30 °C and the $^{13}C\{^1H\}$ NMR spectrum at −40 °C. These spectroscopic data indicate restricted rotation about the W−C bond of the NHC ligand, as well as restricted rotation about the N−C(ipso mesityl) bond. While in many cases NHC ligands rotate freely about the M−C bond, several previous examples of restricted rotation for NHC ligands were observed, with steric hindrance often being cited as the cause.[12,44]

(39) (a) Song, J.-S.; Szalda, D. J.; Bullock, R. M.; Lawrie, C. J. C.; Rodkin, M. A.; Norton, J. R. *Angew. Chem., Int. Ed. Engl.* **1992**, *31*, 1233−1235. (b) Song, J.-S.; Szalda, D. J.; Bullock, R. M. *Organometallics* **2001**, *20*, 3337−3346.

(40) Milke, J.; Missling, C.; Sünkel, K.; Beck, W. *J. Organomet. Chem.* **1993**, *445*, 219−227.

(41) Grundy, K. R.; Robertson, K. N. *Inorg. Chem.* **1985**, *24*, 3898−3903.

(42) Farrow, E.; Sarazin, Y.; Hughes, D. L.; Bochmann, M. *J. Organomet. Chem.* **2004**, *689*, 4624−4629.

(43) Agbossou, S. K.; Smith, W. W.; Gladysz, J. A. *Chem. Ber.* **1990**, *123*, 1293−1299.

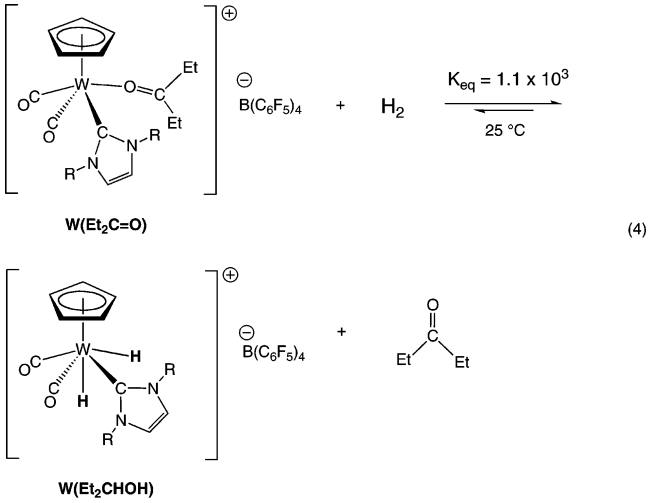

(4)

this temperature was 1.1×10^3. The K_{eq} measured after 1 h at each of these temperatures was the same within experimental uncertainty. Even though the magnitude of the K_{eq} indicates a strong thermodynamic preference for formation of the dihydride from the ketone complex, both species are present under these conditions, due to the much lower concentration of H_2 (9 mM) compared to $Et_2C{=}O$ solvent (9.4 M).

The dihydride **WH_2** is also favored over **W(THF)**; $K_{eq} = [\mathbf{WH_2}][\text{THF-}d_8]/[\mathbf{W(THF\text{-}}d_8\mathbf{)}][H_2] \approx 3 \times 10^3$ in THF-d_8 at 298 K. Solutions of **W(THF-d_8)** eventually become viscous and turn into a gel, likely due to ring opening and oligomerization of the THF-d_8 solvent.

Addition of $Et_2C{=}O$ to a solution of $[CpW(CO)_2(IMes)(Et_2CH{-}OH)]^+[B(C_6F_5)_4]^-$ in C_6D_6 results in displacement of the alcohol by the ketone and formation of $[CpW(CO)_2(IMes)(Et_2C{=}O)]^+[B(C_6F_5)_4]^-$. A lower limit of $K_{eq} > 100$ was estimated for the equilibrium $K_{eq} = [\mathbf{W(Et_2C{=}O)}^+][Et_2CH{-}OH]/[\mathbf{W(Et_2CH{-}OH)}^+][Et_2C{=}O]$, based on an estimated NMR detection limit of 3%. These experiments establish the relative binding strength to $[CpW(CO)_2(IMes)]^+$ as $(H)_2 > Et_2C{=}O > Et_2CH{-}OH$.

Catalytic Hydrogenation of $Et_2C{=}O$. Modest activity for the hydrogenation of $Et_2C{=}O$ (eq 5) is obtained using complexes **W** as the catalyst precursor, which is readily converted into the ketone adduct **W($Et_2C{=}O$)** under these conditions.

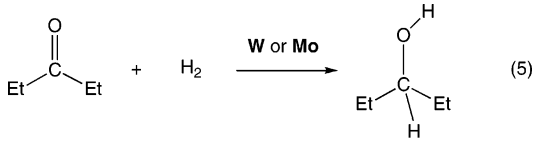

(5)

Catalytic hydrogenation of neat $Et_2C{=}O$ by **W** (0.34 mol %) at 23 °C gives 2.1 turnovers in 1 day at 4 atm H_2 (see Table 1). At higher pressure (54.4 atm H_2), 7.8 turnovers are found after 1 day, and a maximum of 86 turnovers are detected after 10 days. Higher activity is observed at 50 °C (15.1 turnovers in 1 day at 4 atm H_2), but the lifetime of the catalyst decreases. Thus,

Scheme 2

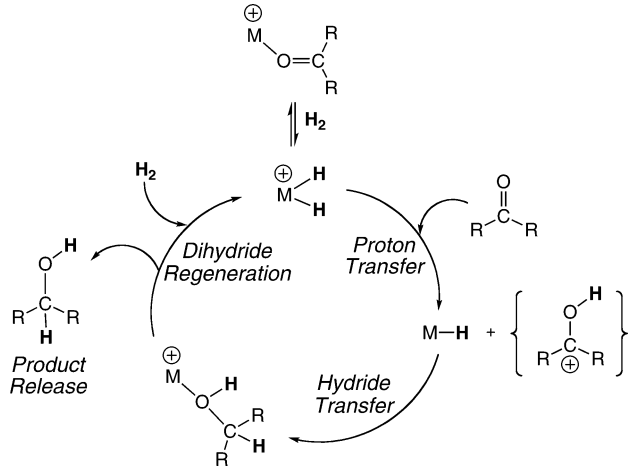

Table 1. Hydrogenation of Neat $Et_2C{=}O$ with 0.34 mol % of Catalyst

catalyst precursor	*T*, °C	pressure, atm	time, h	TON[a]
W	23	4	24	2.1 (0)
W	23	4	238	10.0 (0)
W	50	4	23	15.1 (0.4)
W	50	4	164	29.9 (0.7)
W	23	54.4	24	7.8 (0.2)
W	23	54.4	240	86.0 (6.0)
W	50	54.4	24	15.9 (3.8)
W	50	54.4	168	60.9 (12.6)
Mo	23	4	24	0.9 (0)
Mo	23	4	240	0.9 (0)
Mo	50	4	24	0.8 (0)
Mo	50	4	240	1.0 (0)

[a] Turnover number (TON) is the total number of moles of 3-pentanone hydrogenated per mole of catalyst. It includes TON for the formation of the direct hydrogenation product, 3-pentanol, and the secondary condensation product, $(Et_2CH)_2O$. Each equivalent of the ether is counted as two turnovers of the catalyst, since it is formed from 2 equiv of the alcohol. The number in parentheses is a TON for the ether alone.

10% decomposition is observed in 1 day at 23 °C and 30% in 10 days. At 50 °C, 30% decomposition occurs in 1 day and >97% of the catalyst has decomposed after 7 days. The catalytic activity of **Mo** (~1 turnover in 1 day at 23 °C, 4 atm H_2) is lower than that of **W**, in contrast to the trend observed for phosphine-containing catalysts $CpM(CO)_2(PR_3)(Et_2C{=}O)^+$, where the Mo catalysts were notably more active than the W analogues.[3,4] Complex **Mo** is less stable under hydrogenation conditions. Since only one turnover was obtained, strictly speaking, the Mo complex is not a catalyst.

The proposed mechanism of ionic hydrogenation of ketones by Mo or W catalysts (Scheme 2) involves displacement of a bound ketone by H_2 as the first step (eq 4, discussed above), followed by proton and hydride transfer reactions from metal hydride complexes, as previously outlined[3,4] for Mo and W catalysts reported earlier.

Catalyst Deactivation and Formation of $[H(IMes)]^+$. Vulnerability of Metal−NHC Catalysts. Decomposition of the molybdenum and tungsten catalysts was found to produce multiple metal species, but only one species containing IMes, as judged by the ^1H NMR spectrum. The single product containing the IMes entity was isolated and identified as $[H(IMes)]^+B(C_6F_5)_4^-$ (cf. Scheme 1). It was probed for activity under ionic hydrogenation conditions, but proved to be inactive. The formation of the protonated form of IMes highlights a susceptibility of these catalysts to decomposition. Our experiments do not distinguish a reductive elimination process that

(44) (a) Doyle, M. J.; Lappert, M. F. *J. Chem. Soc., Chem. Commun.* **1974**, 679−680. (b) Herrmann, W. A.; Goossen, L. J.; Spiegler, M. *J. Organomet. Chem.* **1997**, *547*, 357−366. (c) Weskamp, T.; Schattenmann, W. C.; Spiegler, M.; Herrmann, W. A. *Angew. Chem., Int. Ed.* **1998**, *37*, 2490−2493. (d) Enders, D.; Gielen, H. *J. Organomet. Chem.* **2001**, *617*−*618*, 70−80. (e) Chianese, A. R.; Li, X.; Janzen, M. C.; Faller, J. W.; Crabtree, R. H. *Organometallics* **2003**, *22*, 1663−1667. (f) Dinger, M. B.; Nieczypor, P.; Mol, J. C. *Organometallics* **2003**, *22*, 5291−5296. (g) Silva, L. C.; Gomes, P. T.; Veiros, L. F.; Pascu, S. I.; Duarte, M. T.; Namorado, S.; Ascenso, J. R.; Dias, A. R. *Organometallics* **2006**, *25*, 4391−4403.

forms the imidazolium cation from other possible mechanisms. Mechanistic studies would be complicated by the low concentration of the metal complexes under catalytic conditions, together with the formation of more than one metal-containing decomposition product.

In our earlier studies on catalytic reactions using $[Cp(CO)_2(PR_3)M(O{=}CEt_2)]^+BAr'_4{}^-$ as catalyst precursors for the ionic hydrogenation of ketones[3] decomposition to phosphonium cations, HPR_3^+, was identified as a catalyst deactivation pathway. The higher binding strength of NHC ligands versus phosphines was a primary motivation for comparing the reactivity of these new NHC complexes to those with phosphine ligands. More research will be needed to tune the stability properties of these catalysts for hydrogenations, to decrease the susceptibility to proton-mediated decomposition. In contrast to these hydrogenations, hydrosilylation of ketones catalyzed by **W(Et$_2$C=O)** gives much longer catalyst lifetimes.[45] In the case of hydrosilylation of aliphatic ketones, a readily recyclable catalyst is obtained that produces over 1000 total turnovers. Comparison of the catalyst lifetimes for hydrogenation versus hydrosilylation is complicated by the different conditions being used, as the hydrosilylation reactions were all conducted at room temperature, whereas many of the hydrogenations were carried out at 50 °C. Some of the enhanced stability for hydrosilylation may be due to more catalyst decomposition occurring at the higher temperatures employed in the hydrogenation reactions. The longer lifetime of the hydrosilylation catalysts may also be related to the reactivity of the silyl hydride complex $[CpW(CO)_2(IMes)(SiEt_3)H]^+$ compared to the dihydride complex **WH$_2$**. Further studies on the chemical properties and acidities of these complexes would be needed to better understand the differences in catalyst stability.

Previously reported metal−NHC complexes demonstrated a wide range of reactivity (or lack thereof) with acids. For example, Haynes and co-workers found that the Rh−C bond of Rh(I)(NHC)(CO) was cleaved by HCl.[46] In contrast, Crabtree, Faller, and co-workers found that HOAc did not induce any Pd−C bond cleavage of a Pd(NHC) complex, even after 16 h at 55 °C.[29] Herrmann and co-workers reported Pd(II) catalysts for the activation of methane. Their catalytic reaction was carried out at 80−100 °C in CF_3CO_2H, using a Pd complex that had a chelating bis-(NHC)carbene ligand that demonstrates remarkable stability toward acid.[47]

Recent studies have provided an improved understanding of the ways in which metal complexes with NHC ligands decompose.[48] Examples in which alkyl groups on NHC ligands react (often by C−H activation pathways) were mentioned in the Introduction. Such pathways alter the structure of the NHC ligand, but generally leave the M−C bond of the NHC intact. The decomposition pathway we found is less common, resulting in loss of the NHC ligand from the metal. Related reactions that produce imidazolium cations have been reported. Cavell and co-workers have reported kinetic and computational studies on the reactivity of Pd NHC complexes. They reported that $[Pd(CH_3)(tmiy)(PR_3)_2]^+BF_4^-$ complexes (tmiy = 1,3,4,5-tetramethylimidazole-2-ylidene) decompose by a reductive elimination reaction that follows first-order kinetics to produce pentamethylimidazolium and Pd(0) products.[49] Computational studies have explored the geometrical influences on the reductive elimination[50] and the effect of electronic and steric factors on the barrier for elimination.[51] Attempted catalytic olefin hydroformylation using $Co_2(CO)_6(IMes)_2$ led to a decomposition product thought to be $[H(IMes)]^+[Co(CO)_4]^-$.[52]

Conclusions. The NHC-substituted Mo and W hydrides $CpM(CO)_2(IMes)H$ are synthesized in good yield by a displacement of the phosphine in $CpM(CO)_2(PR_3)H$ by IMes. In most cases the initially observed reactivity leads to ionic complexes, $[H(IMes)]^+[CpM(CO)_2(PR_3)]^-$, arising from deprotonation of the metal hydride by the highly basic free NHC. Hydride abstraction from $CpW(CO)_2(IMes)H$ gives $CpW(CO)_2(IMes)^+B(C_6F_5)_4^-$, in which the IMes ligand is a hemilabile bidentate ligand, with one C=C bond of the arene weakly bonding to the metal. Ketones or alcohols readily displace the weak C=C bond, producing $[CpW(CO)_2(IMes)(Et_2C{=}O)]^+$ or $[CpM(CO)_2(IMes)(Et_2CH{-}OH)]^+$. Displacement of the ketone or alcohol by H_2 leads to the dihydride complex $[CpW(CO)_2(IMes)(H)_2]^+$. These W complexes are catalyst precursors for the hydrogenation of neat $Et_2C{=}O$, but activities are modest, and decomposition of the catalyst occurs. The product of the catalyst decomposition is $[H(IMes)]^+$, resulting from protonation of the NHC ligand, exposing a vulnerability of the NHC ligand in this catalytic reaction.

Experimental Section

All manipulations were performed in Schlenk-type glassware on a dual-manifold Schlenk line or in an argon-filled Vacuum Atmospheres glovebox. NMR spectra were obtained on a Bruker Avance 400 FT NMR spectrometer (400 MHz for ^{1}H). All NMR spectra were recorded at 25 °C unless stated otherwise. Chemical shifts for ^{1}H and ^{13}C NMR spectra were referenced using internal solvent resonances and are reported relative to tetramethylsilane. External standards of trifluorotoluene (set as $\delta = -63.73$) and 85% H_3PO_4 (set as $\delta = 0$) were used for referencing ^{19}F and ^{31}P NMR spectra. $^{13}C\{^1H\}$ and $^{31}P\{^1H\}$ NMR spectra were recorded with broadband ^{1}H decoupling unless stated otherwise. For quantitative ^{1}H NMR measurements the relaxation delay was set at 30 s. NMR measurements performed in non-deuterated solvents (e.g., $Et_2C{=}O$) contained sealed capillaries of deuterated solvents (CD_2Cl_2), the spectrometer was locked on the deuterated solvent, and the chemical shift reference used the deuterated solvent. The chemical shifts referenced against standards in sealed capillaries can be substantially different (ca. 1 ppm) from the values obtained by conventional referencing against standards dissolved in the bulk of the sample. Large solvent peaks for the resonances of the solvent obscure some parts of the spectrum from 1 to 3 ppm, but pertinent regions of the spectrum (e.g., Cp, vinyl, and aromatic resonances) can be reliably observed and integrated. GC-MS spectra were recorded on an Agilent Technologies 5973 mass selective detector connected to an Agilent Technologies 6890N gas chromatograph equipped with an HP-5ms column (5% phenyldimethylpolysiloxane). Infrared spectra were recorded on a Mattson Polaris or ThermoNicolet FTIR spectrometer. Elemental analyses were performed by Schwarzkopf Microanalytical Laboratory, Inc. (Woodside, NY) or Atlantic Microlab, Inc. (Norcross, GA).

Hydrocarbon solvents were dried over Na/K-benzophenone. Benzene-d_6 was dried over Na/K. 3-Pentanone was dried over CaH_2.

(45) Dioumaev, V. K.; Bullock, R. M. *Nature* **2003**, *424*, 530−532.
(46) Martin, H. C.; James, N. H.; Aitken, J.; Gaunt, J. A.; Adams, H.; Haynes, A. *Organometallics* **2003**, *22*, 4451−4458.
(47) Muehlhofer, M.; Strassner, T.; Herrmann, W. A. *Angew. Chem., Int. Ed.* **2002**, *41*, 1745−1747.
(48) Crudden, C. M.; Allen, D. P. *Coord. Chem. Rev.* **2004**, *248*, 2247−2273.
(49) McGuinness, D. S.; Saendig, N.; Yates, B. F.; Cavell, K. J. *J. Am. Chem. Soc.* **2001**, *123*, 4029−4040.
(50) Graham, D. C.; Cavell, K. J.; Yates, B. F. *Dalton Trans.* **2005**, 1093−1100.
(51) Graham, D. C.; Cavell, K. J.; Yates, B. F. *Dalton Trans.* **2006**, 1768−1775.
(52) van Rensburg, H.; Tooze, R. P.; Foster, D. F.; Slawin, A. M. Z. *Inorg. Chem.* **2004**, *43*, 2468−2470.

CF_3Ph was vacuum transferred from $LiAlH_4$. H_2 was used as received. 1,3-bis(2,4,6-trimethylphenyl)imidazol-2-ylidene (IMes),[53] $CpMo(CO)_2(PPh_3)H$,[54] $CpMo(CO)_2(PMe_3)H$,[55] $CpW(CO)_2(PPh_3)H$,[54] and $CpW(CO)_2(PMe_3)H$[55] were synthesized according to the literature procedures. A sample of $Ph_3C^+B(C_6F_5)_4^-$ was donated by Albemarle Corporation.

Simulations of the dynamic NMR spectra were carried out using the gNMR software package (v3.6.5 for Macintosh, Cherwell Scientific Publishing Limited). The rates of exchange as a function of temperature were determined from visual comparison of the experimental and simulated spectra. The errors in the rate constants of ca. 10% were estimated on the basis of subjective judgments of the sensitivity of the fits to changes in the rate constants. The temperature of the NMR probe was calibrated using methanol.[56] The activation parameters and their uncertainties were calculated using KINPAR, a Macintosh computer program provided by Prof. Jack Norton (Columbia University).

Synthesis of *cis*-$CpMo(CO)_2$(IMes)H from $CpMo(CO)_2(PPh_3)H$. In a glovebox $CpMo(CO)_2(PPh_3)H$ (480.0 mg, 1.000 mmol), IMes (306.0 mg, 1.000 mmol), and 10 mL of toluene were placed in a glass tube equipped with a Teflon valve. The light yellow solids dissolved to produce a dark purple solution, and a new light yellow precipitate formed almost immediately. The tube was heated at 95 °C for 3 h. The product was recrystallized from toluene−hexanes (1:3) to yield 449 mg (86%) of pure $CpMo(CO)_2$(IMes)H as light yellow crystals. ^{1}H NMR (THF-d_8): δ 7.16 (s, 2H, =C*H*), 7.02 (s, 4H, *m-H*-Mes), 4.62 (s, 5H, *Cp*), 2.34 (s, 6H, *p-Me*-Mes), 2.09 (s, 12H, *o-Me*-Mes), −4.73 (s, 1H, Mo*H*). ^{13}C NMR (THF-d_8; some assignments were aided by recording ^{13}C APT (attached proton test) experiments): δ 243.3 (d, $^2J_{CH}$ = 11 Hz, Mo-*C*O), 200.2 (d, $^2J_{CH}$ = 12 Hz, N*C*N), 139.5 (m, *i-Mes*), 139.2 (q, $^2J_{CH}$ = 6 Hz, *p-Mes*), 136.9 (q, $^2J_{CH}$ = 6 Hz, o-*Mes*), 130.0 (dm, $^1J_{CH}$ = 156 Hz, *m-Mes*), 124.3 (dd, $^1J_{CH}$ = 196 and $^2J_{CH}$ = 12 Hz, =*C*H), 89.0 (d of quintets, $^1J_{CH}$ = 174 and J_{CH} = 6 Hz, *Cp*), 21.2 (qt, $^1J_{CH}$ = 126 and $^3J_{CH}$ = 4 Hz, *p-Me*-Mes), 18.8 (qm, $^1J_{CH}$ = 128 Hz, *o-Me*-Mes). IR (THF-d_8): ν_{sym}(CO) 1918 (vs), ν_{asym}(CO) 1843 (vs) cm^{-1}, I_{asym}/I_{sym} = 1.0 (predicted OC−Mo−CO angle 90°). IR (hexanes): ν_{sym}(CO) 1930 (vs), ν_{asym}(CO) 1858 (vs) cm^{-1}, I_{asym}/I_{sym} = 0.93 (predicted OC−Mo−CO angle 88°). Anal. Calcd for $C_{28}H_{30}N_2O_2Mo$: C, 64.37; H, 5.79; N, 5.36. Found: C, 64.13; H, 6.05; N, 5.34.

$CpMo(CO)_2(PPh_3)^-(H^+$IMes). $CpMo(CO)_2(PPh_3)H$ (306 mg, 0.64 mmol) and IMes (194 mg, 0.64 mmol) were charged into a 100 mL flask, and toluene (20 mL) was added, giving an orange solution. After stirring at 23 °C for 10 min, hexane (40 mL) was added, and an orange precipitate formed immediately. The precipitate was washed with hexane (3 × 10 mL) and dried under vacuum to give an orange solid (409 mg, 82%). Anal. Calcd for $C_{46}H_{45}N_2O_2PMo$: C, 70.40; H, 5.78; N, 3.57. Found: C, 70.13; H, 6.01; N, 3.08. ^{1}H NMR (C_6D_6, 23 °C): δ 10.82 (br s, 1H, *H*CN_2), 7.89 (t m, J_{HH} = 8 Hz, 6H, *PPh*), 6.98 (m, 9H, *PPh*), 6.70 (s, 4H, *m-H*-Mes), 5.97 (s, 2H, =C*H*), 4.71 (s, 5H, *Cp*), 2.09 (s, 6H, *p-Me*-Mes), 1.98 (s, 12H, *o-Me*-Mes). ^{31}P NMR (C_6D_6, 23 °C): δ 89.7 (s, *P*Ph_3). ^{13}C{^{1}H} NMR (C_6D_6, 23 °C): δ 243.0 (Mo-*C*O), 242.9 (Mo-*C*O), 159.6 (N*C*N), 145.7 (d, *i*-P*Ph*$_3$, J = 30), 141.3 (*i-Mes*), 135.3 (*p*-P*Ph*$_3$), 134.2 (d, *o*-P*Ph*$_3$, J = 13), 132.0 (*p-Mes*), 130.2 (o-*Mes*), 127.5 (d, *m*-P*Ph*$_3$, J = 8), 127.4 (*m-Mes*), 124.1 (=*C*H), 86.3 (*Cp*), 21.5 (*p-Me*-Mes), 17.8 (*o-Me*-Mes). ^{1}H NMR (THF-d_8): δ 10.44 (br s, 1H, *H*CN_2), 7.85 (s, 2H, =C*H*), 7.43 (m, 6H, *PPh*), 7.12 (s, 4H, *m-H*-Mes), 7.01 (m, 9H, *PPh*), 4.20 (s, 5H, *Cp*), 2.38 (s, 6H, *p-Me*-Mes), 2.19 (s, 12H, *o-Me*-Mes). ^{31}P NMR (THF-d_8): δ 87.9 (s, *P*Ph_3). ^{1}H NMR (CD_3CN): δ 8.73 (br s, 1H, *H*CN_2), 7.71 (s, 2H, =C*H*), 7.51 (m, 6H, *PPh*), 7.22 (m, 9H, *PPh*), 7.17 (s, 4H, *m-H*-Mes), 4.67 (s, 5H, *Cp*), 2.38 (s, 6H, *p-Me*-Mes), 2.13 (s, 12H, *o-Me*-Mes). ^{31}P NMR (THF-d_8): δ 89.0 (s, *P*Ph_3). IR data: IR (C_6D_6): ν_{sym}(CO) 1778 (vs), ν_{asym}(CO) 1700 (vs) cm^{-1}, I_{asym}/I_{sym} = 1.20 (predicted OC−W−CO angle 95°). IR (THF-d_8): ν_{sym}(CO) 1785 (vs), ν_{asym}(CO) 1707 (vs) cm^{-1}, I_{asym}/I_{sym} = 1.18 (predicted OC−W−CO angle 94°).

Observation of $CpMo(CO)_2(PMe_3)^-$[H(IMes)]$^+$ in the Reaction of $CpMo(CO)_2(PMe_3)H$ with IMes. $CpMo(CO)_2(PMe_3)H$ (2.9 mg, 0.01 mmol), IMes (3.1 mg, 0.01 mmol), and 0.6 mL of C_6D_6 were placed in an NMR tube equipped with a Teflon valve. The light yellow solids dissolved to produce a dark purple solution. ^{1}H NMR spectrum acquired after 5 min at room temperature showed ca. 40% of the starting $CpMo(CO)_2(PMe_3)H$, ca. 20% of $CpMo(CO)_2$(IMes)H + free PMe_3, and ca. 40% of a new product, $CpMo(CO)_2(PMe_3)^-$[H(IMes)]$^+$. ^{1}H NMR (C_6D_6): δ 11.53 (br s, 1H, *H*CN_2), 6.76 (s, 4H, *m-H*-Mes), 6.29 (br s, 2H, =C*H*), 4.92 (br s, 5H, *Cp*), 2.12 (s, 6H, *p-Me*-Mes), 2.11 (s, 12H, *o-Me*-Mes), 1.38 (d, $^2J_{HP}$ = 7 Hz, 9H, *PMe*). ^{31}P NMR (C_6D_6): δ 29.4 (s, *P*Me_3).

Synthesis of $CpW(CO)_2$(IMes)H from $CpW(CO)_2(PMe_3)H$. $CpW(CO)_2(PMe_3)H$ (346.0 mg, 0.900 mmol), IMes (275.0 mg, 0.900 mmol), and toluene (1 mL) were placed in a glass tube equipped with a Teflon valve. The light yellow solids dissolved to produce a dark purple solution, then a new light yellow precipitate formed almost immediately. The volatiles were removed under vacuum, and the residue was heated under vacuum for 10 min at 120 °C to remove free phosphine and reestablish the equilibrium in favor of $CpW(CO)_2$(IMes)H. The product was recrystallized from toluene−hexanes (1:1) to yield pure $CpW(CO)_2$(IMes)H (416 mg, 76%) as light yellow crystals with 0.5 equiv of crystallization solvent ($C_6H_5CH_3$) per W detected by NMR. ^{1}H NMR (C_6D_6): δ 6.80 (s, 4H, *m-H*-Mes), 6.19 (s, 2H, =C*H*), 4.60 (s, 5H, *Cp*), 2.12 (s, 6H, *p-Me*-Mes), 2.10 (s, 12H, *o-Me*-Mes), −5.93 (s, $^1J_{WH}$ = 45 Hz, 1H, W*H*). ^{1}H NMR (THF-d_8, −100 °C): δ 7.40 (s, 2H, =C*H*), 7.06 (s, 4H, *m-H*-Mes), 4.71 (s, 5H, *Cp*), 2.34 (s, 6H, *p-Me*-Mes), 2.12 (br s, 6H, *o-Me*-Mes), 2.01 (br s, 6H, *o-Me*-Mes), −6.43 (s, $^1J_{WH}$ = 45 Hz, 1H, W*H*). ^{13}C NMR (C_6D_6) δ 238.1 (br, W-*C*O), 184.1 (d, $^2J_{CH}$ = 14.8 Hz, N*C*N), 139.1 (m, *i-Mes*), 138.9 (q, $^2J_{CH}$ = 6 Hz, *p-Mes*), 136.6 (q, $^2J_{CH}$ = 6 Hz, o-*Mes*), 129.9 (dm, $^1J_{CH}$ = 157 Hz, *m-Mes*), 122.9 (dd, $^1J_{CH}$ = 195 and $^2J_{CH}$ = 12 Hz, =*C*H), 87.4 (d quintet, $^1J_{CH}$ = 177 and J_{CH} = 7 Hz, *Cp*), 21.4 (qt, $^1J_{CH}$ = 126 and $^3J_{CH}$ = 5 Hz, *p-Me*-Mes), 19.1 (qm, $^1J_{CH}$ = 127 Hz, *o-Me*-Mes). ^{13}C{^{1}H} NMR (THF-d_8, −100 °C): δ 247.4 (br s, W-*C*O), 232.3 (br s, W-*C*O), 181.5 (s, N*C*N), 139.4 (s, *p-Mes* or *i-Mes*), 138.9 (s, *p-Mes* or *i-Mes*), 137.1 (br s, *o-Mes*), 136.6 (br s, *o-Mes*), 129.8 (br s, *m-Mes*), 124.1 (br s, =*C*H), 88.0 (s, *Cp*), 21.3 (br s, *p-Me*-Mes), 19.4 (br s, *o-Me*-Mes), 18.9 (br s, *o-Me*-Mes). IR (toluene): ν_{sym}(CO) 1915 (vs), ν_{asym}(CO) 1824 (vs) cm^{-1}, I_{asym}/I_{sym} = 0.93 (predicted OC−W−CO angle 88°). IR (THF-d_8): ν_{sym}(CO) 1913 (vs), ν_{asym}(CO) 1822 (vs) cm^{-1}, I_{asym}/I_{sym} = 0.90 (predicted OC−W−CO angle 87°). IR (CD_2Cl_2): ν_{sym}(CO) 1906 (vs), ν_{asym}(CO) 1810 (vs) cm^{-1}, I_{asym}/I_{sym} = 0.95 (predicted OC−W−CO angle 89°). Anal. Calcd for $C_{31.5}H_{34}N_2O_2W$ (formula includes 0.5 equiv of crystallization solvent, $C_6H_5CH_3$, per W): C, 57.63; H, 5.22; N, 4.27. Found: C, 57.52; H, 5.07; N, 4.14.

Synthesis of *cis*-$CpW(CO)_2$(IMes)H from $CpW(CO)_2(PPh_3)H$. $CpW(CO)_2(PPh_3)H$ (608 mg, 1.07 mmol), IMes (333 mg, 1.09 mmol), and toluene (3 mL) were placed in a glass tube equipped with a Teflon valve. The yellow solids dissolved to produce a brown-red solution, and a light yellow precipitate formed within 10−20 min. The color faded slowly to yellow-gray, indicating completion of the reaction after 2 days at 23 °C. The product was washed with hexane (2 × 7 mL) and recrystallized from toluene−hexane (1:1) to yield pure $CpW(CO)_2$(IMes)H (568 mg, 87%) as light yellow crystals. The product was identified by comparison to

(53) Arduengo, A. J., III; Dias, H. V. R.; Harlow, R. L.; Kline, M. *J. Am. Chem. Soc.* **1992**, *114*, 5530−5534.

(54) (a) Bainbridge, A.; Craig, P. J.; Green, M. *J. Chem. Soc. (A)* **1968**, 2715−2718. (b) Beck, W.; Schloter, K.; Sünkel, K.; Urban, G. *Inorg. Synth.* **1989**, *26*, 96−106.

(55) Kalck, P.; Pince, R.; Poilblanc, R.; Roussel, J. *J. Organomet. Chem.* **1970**, *24*, 445−452.

(56) Van Geet, A. L. *Anal. Chem.* **1970**, *42*, 679−680.

an authentic sample of $CpW(CO)_2(IMes)H$, which was synthesized by an independent route.

Observation of $CpW(CO)_2(PPh_3)^-[H(IMes)]^+$ Intermediate in the Reaction of $CpW(CO)_2(PPh_3)H$ with IMes. $CpW(CO)_2(PPh_3)H$ (5.7 mg, 0.01 mmol), IMes (3.1 mg, 0.01 mmol), and C_6D_6 (0.6 mL) were placed in an NMR tube equipped with a Teflon valve. The light yellow solids dissolved to produce a brown-red solution. An ^1H NMR spectrum acquired after 5 min at room temperature showed ca. 40% of the starting $CpW(CO)_2(PPh_3)H$ and ca. 60% of a new product, $CpW(CO)_2(PPh_3)^-[H(IMes)]^+$. ^1H NMR (C_6D_6): δ 10.95 (br s, 1H, *H*CN$_2$), 7.88 (t, J_{HH} = 8 Hz, 6H, *PPh*), 6.98 (m, 9H, *PPh*), 6.74 (s, 4H, *m-H*-Mes), 6.23 (s, 2H, =C*H*), 4.61 (s, 5H, *Cp*), 2.12 (s, 6H, *p-Me*-Mes), 2.05 (s, 12H, *o-Me*-Mes).

Synthesis of $[CpMo(CO)_2(IMes)]^+[B(C_6F_5)_4]^-$ (Mo). In a glovebox $CpMo(CO)_2(IMes)H$ (52.4 mg, 0.100 mmol) was added slowly to a stirred solution of $Ph_3C^+B(C_6F_5)_4^-$ (96.6 mg, 0.105 mmol) in toluene (5 mL). A dark purple precipitate formed, and the stirring was continued for 40 min. The bright yellow mother liquor was removed, and the precipitate was washed with toluene until the washings were colorless (5 × 3 mL). The product was washed with hexanes (3 × 3 mL) and dried *in vacuo* to yield dark purple crystals of pure $CpMo(CO)_2(IMes)^+B(C_6F_5)_4^-$ (112 mg, 87%) with 0.5 equiv of crystallization solvent ($C_6H_5CH_3$) per Mo. The product was insoluble in common noncoordinating NMR solvents. For spectra in THF-d_8 see $[CpMo(CO)_2(IMes)(THF\text{-}d_8)]^+[B(C_6F_5)_4]^-$. IR (Nujol): ν_{sym}(CO) 1999 (vs), ν_{asym}(CO) 1905 (vs) cm^{-1}, I_{asym}/I_{sym} = 1.05 (predicted OC−Mo−CO angle 91°). Anal. Calcd for $C_{55.5}H_{33}BF_{20}N_2O_2Mo$ (with 0.5 equiv of crystallization solvent, $C_6H_5CH_3$, per Mo): C, 53.47; H, 2.67; N, 2.25. Found: C, 53.18; H, 2.77; N, 2.43.

***cis*-$[CpMo(CO)_2(IMes)(THF\text{-}d_8)]^+[B(C_6F_5)_4]^-$, Mo(THF-$d_8$).** ^1H NMR (THF-d_8): δ 7.83 (s, 2H, =C*H*), 7.13 (s, 4H, *m-H*-Mes), 5.14 (s, 5H, *Cp*), 2.36 (s, 6H, *p-Me*-Mes), 2.11 (s, 12H, *o-Me*-Mes). $^{13}C\{^1H\}$ NMR (THF-d_8): δ 251 (br, Mo-*C*O), 187.3 (s, N*C*N), 149.3 (dm, $^1J_{CF}$ = 246 Hz, *o*-C_6F_5), 141.0 (br s, *p-Mes* or *i-Mes*), 139.2 (dm, $^1J_{CF}$ = 243 Hz, *p*-C_6F_5), 137.4 (br s, *p-Mes* or *i-Mes*), 137.2 (dm, $^1J_{CF}$ = 244 Hz, *m*-C_6F_5), 136.5 (br s, *o-Mes*), 130.3 (br s, *m-Mes*), 127.6 (br s, =*C*H), 125 (br m, *i*-C_6F_5), 96.9 (s, *Cp*), 21.0 (s, *p-Me*-Mes), 18.7 (br s, *o-Me*-Mes). ^{19}F NMR (THF-d_8) δ −132.9 (d, 8F, $^3J_{FF}$ = 10 Hz, *o*-C_6F_5), −165.1 (t, 4F, $^3J_{FF}$ = 21 Hz, *p*-C_6F_5), −168.6 (t, 8F, $^3J_{FF}$ = 18 Hz, *m*-C_6F_5). IR (THF): ν_{sym}(CO) 1977 (vs), ν_{asym}(CO) 1882 (vs) cm^{-1}, I_{asym}/I_{sym} = 1.15 (predicted OC−Mo−CO angle 94°).

Synthesis of $[CpW(CO)_2(IMes)]^+[B(C_6F_5)_4]^-$ (W). In a glovebox $CpW(CO)_2(IMes)H$ (244.0 mg, 0.400 mmol) was added slowly to a stirred solution of $Ph_3C^+B(C_6F_5)_4^-$ (387.0 mg, 0.420 mmol) in 10 mL of toluene, and a dark purple precipitate formed. The stirring was continued for 30 min. The bright yellow mother liquor was discarded, and the precipitate was washed with toluene until the washings were colorless (5 × 3 mL). The product was washed with hexanes (3 × 3 mL) and dried under vacuum to yield dark purple crystals of pure $[CpW(CO)_2(IMes)]^+[B(C_6F_5)_4]^-$ (490 mg, 91%) with 1 equiv of crystallization solvent ($C_6H_5CH_3$) per W. The product was insoluble in common noncoordinating NMR solvents. For spectra in THF-d_8 see $[CpW(CO)_2(IMes)(THF\text{-}d_8)]^+[B(C_6F_5)_4]^-$. ^1H NMR (CF_3Ph and a sealed capillary of C_6D_6 for lock): δ 6.76 (br s, 4H, *m-H*-Mes), 6.66 (br s, 2H, =C*H*), 5.13 (br s, 5H, *Cp*), 2.09 (s, 6H, *p-Me*-Mes), 2.06 (s, 12H, *o-Me*-Mes). IR (Nujol): ν_{sym}(CO) 1980 (vs), ν_{asym}(CO) 1890 (vs) cm^{-1}. IR (CF_3-Ph): ν_{sym}(CO) 1983 (vs), ν_{asym}(CO) 1900 (vs) cm^{-1}. Anal. Calcd for $C_{59}H_{37}BF_{20}N_2O_2W$ (formula includes 1 equiv of crystallization solvent, $C_6H_5CH_3$, per W): C, 51.33; H, 2.70; N, 2.03. Found: C, 51.24; H, 3.35; N, 2.02. Single crystals of $CpW(CO)_2(IMes)^+B(C_6F_5)_4^-$ were grown directly from the reaction mixture by slow diffusion of reagents.

***cis*-$[CpW(CO)_2(IMes)(THF\text{-}d_8)]^+[B(C_6F_5)_4]^-$.** ^1H NMR (THF-d_8, −30 °C): δ 7.99 and 7.87 (d, $^1J_{HH}$ = 2 Hz, 1H, =C*H*), 7.26, 7.19, 7.16, and 7.03 (s, 1H, *m-H*-Mes), 5.36 (s, 5H, *Cp*), 2.41, 2.31, 2.30, 2.23, 2.14, and 2.02 (s, 3H, *p-Me*-Mes and *o-Me*-Mes). $^{13}C\{^1H\}$ NMR (THF-d_8, −40 °C): δ 247.1 and 246.2 (s, W-*C*O), 179.6 (s, N*C*N), 149.0 (br d, $^1J_{CF}$ = 240 Hz, *o*-C_6F_5), 141.3 and 140.0 (s, *p-Mes* or *i-Mes*), 139.1 (dm, $^1J_{CF}$ = 242 Hz, *p*-C_6F_5), 137.9 (s, *p-Mes* or *i-Mes*), 137.0 (dm, $^1J_{CF}$ = 244 Hz, *m*-C_6F_5), 137.5, 136.7, 136.5, and 135.8 (s, *o-Mes*), 130.7, 130.3, 130.2, and 129.4 (s, *m-Mes*), 128.4 and 126.6 (br s, =*C*H), 125 (br m, *i*-C_6F_5), 95.4 (s, *Cp*), 21.1 and 21.0 (s, *p-Me*-Mes), 19.7, 18.9, 18.7, and 18.6 (s, *o-Me*-Mes). ^{19}F NMR (THF-d_8, −30 °C): δ −133.5 (d, 8F, $^3J_{FF}$ = 11 Hz, *o*-C_6F_5), −164.9 (t, 4F, $^3J_{FF}$ = 21 Hz, *p*-C_6F_5), −168.5 (t, 8F, $^3J_{FF}$ = 18 Hz, *m*-C_6F_5). IR (THF-d_8): ν_{sym}(CO) 1962 (vs), ν_{asym}(CO) 1859 (vs) cm^{-1}, I_{asym}/I_{sym} = 1.06 (predicted OC−W−CO angle 92°).

$[CpW(CO)_2(IMes)(H)_2]^+[B(C_6F_5)_4]^-$ (WH_2). $[CpW(CO)_2(IMes)]^+[B(C_6F_5)_4]^-\cdot CH_3Ph$ (30 mg, 0.022 mmol) was suspended in toluene (5 mL) and placed in a tube equipped with a Teflon valve. The tube was filled with about 1.1 atm H_2 at −196 °C, sealed, and warmed to room temperature with vigorous stirring. The color of the suspension changed almost immediately from brown to yellow. The supernatant was removed, and the precipitate was dried under vacuum to yield pure $[CpW(CO)_2(IMes)(H)_2]^+[B(C_6F_5)_4]^-$ (25 mg, 91%) as a yellow powder. The sample suspended in C_6D_6 was found to contain $[CpW(CO)_2(IMes)(H)_2]^+[B(C_6F_5)_4]^-$ and 1 equiv of toluene. Anal. Calcd for $C_{59}H_{39}BF_{20}N_2O_2W$ (formula includes 1 equiv of $C_6H_5CH_3$, per W): C, 51.25; H, 2.84; N, 2.03. Found: C, 51.03; H, 2.68; N, 2.17. ^1H NMR (C_6D_6, 23 °C): δ 6.71 (s, 4H, *m*-H-Mes), 5.94 (s, 2H, =C*H*), 4.09 (s, 5H, *Cp*), 2.09 (s, 6H, *p*-Me-Mes), 1.58 (s, 12H, *o*-Me-Mes), −1.15 (br s, $\nu_{1/2}$ = 14 Hz 2H, W*H*). The low solubility in C_6D_6 precluded reliable ^{13}C NMR measurements. ^1H NMR (THF-d_8, −40 °C): δ 7.82 (s, 2H, =C*H*), 7.17 (s, 4H, *m*-H-Mes), 5.46 (s, 5H, *Cp*), 2.37 (s, 6H, *p*-Me-Mes), 2.06 (s, 12H, *o*-Me-Mes), −0.7 (br s, $\nu_{1/2}$ = 1400 Hz, 2H, W*H*). ^1H NMR (THF-d_8, −100 °C): δ 7.95 (s, 2H, =C*H*), 7.19 (s, 4H, *m*-H-Mes), 5.59 (s, 5H, *Cp*), 2.38 (s, 6H, *p*-Me-Mes), 2.07 (s, 12H, *o*-Me-Mes), 1.19 (br s, $\nu_{1/2}$ = 13 Hz, 1H, W*H*), −2.97 (∼br d, $\nu_{1/2}$ = 12 Hz, $^2J_{HH}$ = 3 Hz, $^1J_{HW}$ = 34 Hz, 1H, W*H*). $^{13}C\{^1H\}$ NMR (THF-d_8, −100 °C): δ 205.2 and 203.1 (s, W-*C*O), 160.7 (s, N*C*N), 148.8 (br d, $^1J_{CF}$ = 242 Hz, *o*-C_6F_5), 141.0 (br s, *p*-Mes or *i*-Mes), 139.0 (dm, $^1J_{CF}$ = 242 Hz, *p*-C_6F_5), 138.5 (s, *p*-Mes or *i*-Mes), 137.0 (dm, $^1J_{CF}$ = 247 Hz, *m*-C_6F_5), 136.4 (br s, o-Mes), 130.6 and 130.5 (s, *m*-Mes), 127.9 (br s, =*C*H), 124.5 (br m, *i*-C_6F_5), 88.6 (s, *Cp*), 21.2 (s, *p*-Me-Mes), 18.7 and 18.3 (s, *o*-Me-Mes). ^{19}F NMR (THF-d_8, −40 °C): δ −133.5 (d, 8F, $^3J_{FF}$ = 11 Hz, *o*-C_6F_5), −164.9 (t, 4F, $^3J_{FF}$ = 21 Hz, *p*-C_6F_5), −168.5 (t, 8F, $^3J_{FF}$ = 18 Hz, *m*-C_6F_5). $[CpW(CO)_2(IMes)(H)_2]^+[B(C_6F_5)_4]^-$ is not stable in THF-d_8 at 23 °C; $[CpW(CO)_2(IMes)(THF\text{-}d_8)]^+[B(C_6F_5)_4]^-$ started to form. Additionally, $[CpW(CO)_2(IMes)(THF\text{-}d_8)]^+[B(C_6F_5)_4]^-$ does not react with H_2 in THF-d_8 at 23 °C. IR (Nujol): ν_{sym}(CO) 2073 (vs), ν_{asym}(CO) 2018 (vs) cm^{-1}, I_{asym}/I_{sym} = 1.18 (predicted OC−W−CO angle 95°). IR (C_6D_6): ν_{sym}(CO) 2065 (w), ν_{asym}(CO) 2006 (w) cm^{-1}.

$[CpW(CO)_2(IMes)(Et_2C{=}O)]^+[B(C_6F_5)_4]^-$, W($Et_2C$=O). $[CpW(CO)_2(IMes)]^+[B(C_6F_5)_4]^-\cdot CH_3Ph$ (53 mg, 0.038 mmol) and Et_2C=O (300 μL, 2.83 mmol) were mixed to produce a dark purple solution and placed in an NMR tube equipped with a Teflon valve. The volatiles were removed *in vacuo*, giving $[CpW(CO)_2(IMes)(Et_2C{=}O)]^+[B(C_6F_5)_4]^-$ as a purple product. ^1H NMR (C_6D_6): δ 6.6 (br s, 4H, *m*-H-Mes), 6.10 (s, 2H, =C*H*), 4.49 (s, 5H, *Cp*), 2.08 (s, 6H, *p*-Me-Mes), 1.9 (br s, 4H, CH_3CH_2), 1.70 (br s, 12H, *o*-Me-Mes), 0.72 (br s, 6H, CH_3CH_2). $^{13}C\{^1H\}$ NMR (Et_2C=O and a sealed capillary of CD_2Cl_2 for lock, −30 °C): δ 248.1 and 246.4 (s, W-*C*O), 241.1 (s, Et_2C=O), 177.4 (s, N*C*N), 148.7 (dm, $^1J_{CF}$ = 244 Hz, *o*C_6F_5), 140.8 (br s, *p-Mes* or *i-Mes*), 138.7 (dm, $^1J_{CF}$ = 247 Hz, *p*-C_6F_5), 136.9 (s, *p-Mes* or *i-Mes*),

136.7 (dm, $^1J_{CF}$ = 247 Hz, *m*-C_6F_5), 136.7 (s, o-*Mes*), 130.2 (s, *m*-*Mes*), 128 and 126 (v b, =*C*H tentative assignment), 124.6 (br m, *i*-C_6F_5), 96.0 (s, *Cp*), 37.8 (s, CH_3CH_2), 21.0 (s, *p*-*Me*-Mes), 18.8, 18.6, and 17.9 (s, *o*-*Me*-Mes), 8.9 (s, CH_3CH_2). ^{19}F NMR δ (Et_2C=O and a sealed capillary of CD_2Cl_2 for lock, −30 °C): −133.3 (dm, 8F, $^3J_{FF}$ = 11 Hz, *o*-C_6F_5), −164.3 (tm, 4F, $^3J_{FF}$ = 21 Hz, *p*-C_6F_5), −168.2 (tm, 8F, $^3J_{FF}$ = 17 Hz, *m*-C_6F_5). IR (Et_2C=O): ν_{sym}(CO) 1960 (vs), ν_{asym}(CO) 1859 (vs) cm^{-1}, W(Et_2C=O) carbonyl band is obscured by the solvent, I_{asym}/I_{sym} = 1.22 (predicted OC−W−CO angle 96°). IR (C_6D_6): ν_{sym}(CO) 1959 (vs), ν_{asym}(CO) 1857 (vs) cm^{-1}, ν(C=O) = 1717 (w) cm^{-1}, low solubility precludes reliable determination of relative intensities. UV(toluene): λ_{max} = 498 nm ($\epsilon = 1 \times 10^3$ L mol^{-1} cm^{-1}).

[CpW(CO)$_2$(IMes)(Et_2CH−OH)]$^+$[B(C_6F_5)$_4$]$^-$, W(Et_2CHOH). [CpW(CO)$_2$(IMes)]$^+$[B(C_6F_5)$_4$]$^-$·CH_3Ph (85 mg, 0.062 mmol) was suspended in C_6H_6 (5 mL), and Et_2CH−OH (50 μL, 0.46 mmol) was added. All the solid dissolved to yield a purple solution, which was stirred for another hour. This solution was then maintained at 23 °C without stirring. After 2 days, a purple crystalline solid formed at the bottom of the flask. The supernatant was carefully decanted, and the solid was washed with hexanes (2 × 5 mL) and C_6H_6 (1 mL) and dried under vacuum for 30 min. [CpW(CO)$_2$(IMes)(Et_2CH−OH)]$^+$[B(C_6F_5)$_4$]$^-$ (55 mg, 65%) was collected as a purple crystalline solid. X-ray-quality crystals were obtained, and the structure was determined by high-intensity X-ray radiation at the National Synchrotron Light Source. ^{1}H NMR (C_6D_6): δ 6.53 (br s, 4H, *m*-H-Mes), 5.89 (br s, 2H, =C*H*), 4.66 (br s, 5H, *Cp*), 3.12 (br s, 1H, C*H*-OH), 1.98 (br s, 6H, *p*-Me-Mes), 1.83 (br s, 12H, *o*-Me-Mes), 1.22 (br s, 4H, CH_3CH_2), 0.79 (br s, 6H, CH_3CH_2), 0.62 (br s, 1H, CH−O*H*). ^{19}F NMR (C_6D_6): δ −131.7 (d, 8F, $^3J_{FF}$ = 11 Hz, *o*-C_6F_5), −162.3 (t, 4F, $^3J_{FF}$ = 21 Hz, *p*-C_6F_5), −166.2 (t, 8F, $^3J_{FF}$ = 18 Hz, *m*-C_6F_5). The low solubility in C_6D_6 precluded reliable ^{13}C NMR measurements. IR (C_6D_6): ν_{sym}(CO) 1973 (vs), ν_{asym}(CO) 1891 (vs) cm^{-1}, I_{asym}/I_{sym} = 0.79 (predicted OC−W−CO angle 83°).

For comparison, ^{1}H NMR of free Et_2CH−OH in C_6D_6 ([Et_2CH−OH] = 0.037 M) was obtained at 23 °C. ^{1}H NMR (C_6D_6): δ 3.14 (m, 1H, C*H*-OH), 1.24 (m, 4H, CH_3CH_2), 0.82 (t, $^3J_{HH}$ = 8 Hz, 6H, CH_3CH_2), 0.67 (d, 1H, $^3J_{HH}$ = 5 Hz, CH-O*H*).

Isolation of [H(IMes)]$^+$B(C_6F_5)$_4$]$^-$. The Mo-catalyzed hydrogenation mixture described above (300 mM Et_2C=O in C_6D_6) was heated for 30 min at 100 °C to complete catalyst decomposition. The colorless precipitate was separated, dried under vacuum, and redissolved in THF-d_8. ^{1}H NMR (THF-d_8): δ 9.24 (t, $^1J_{HH}$ = 2 Hz, 1H, *H*CN$_2$), 8.06 (d, $^1J_{HH}$ = 2 Hz, 2H, =C*H*), 7.19 (s, 4H, *m*-*H*-Mes), 2.37 (s, 6H, *p*-*Me*-Mes), 2.17 (s, 12H, *o*-*Me*-Mes). ^{13}C-{^{1}H} NMR (THF-d_8): δ 142.8 (s, *p*-*Mes* or *i*-*Mes*), 138.2 (s, *p*-*Mes* or *i*-*Mes*), 135.3 (s, o-*Mes*), 132.0 (s, N*C*N), 130.7 (s, *m*-*Mes*), 126.3 (s, =*C*H), 21.1 (s, *p*-*Me*-Mes), 17.3 (s, *o*-*Me*-Mes). Due to the low concentration of the sample, the ^{13}C NMR signals of C_6F_5 were not reliably observed or assigned. ^{19}F NMR (THF-d_8): δ −132.9 (d, 8F, $^3J_{FF}$ = 11 Hz, *o*-C_6F_5), −165.3 (t, 4F, $^3J_{FF}$ = 21 Hz, *p*-C_6F_5), −168.8 (t, 8F, $^3J_{FF}$ = 17 Hz, *m*-C_6F_5).

Comparative Substrate (Et_2C=O, Et_2CH−OH, and H_2) Coordination. The relative binding strength of various substrates (Et_2C=O, Et_2CH−OH, and H_2) is important in the catalytic ionic hydrogenation reactivity and was compared using the CpW(CO)$_2$(IMes)$^+$ system.

The measurement is illustrated by the following example of Et_2CH−OH and Et_2C=O at 23 °C: [CpW(CO)$_2$(IMes)(Et_2CH−OH)]$^+$[B(C_6F_5)$_4$]$^-$ (8.0 mg, 0.006 mmol) was prepared in C_6D_6 (0.6 mL) according to the above procedure, with Et_2CH−OH (13 μL, 0.12 mmol, 20 equiv) present. The ^{1}H NMR spectrum contained one set of broad resonances for Et_2CH−OH, indicative of a fast intermolecular exchange of free and coordinated alcohol on the NMR time scale. Upon addition of Et_2C=O (4.4 μL, 0.042 mmol, 7 equiv), the ^{1}H NMR spectrum showed that [CpW(CO)$_2$(IMes)(Et_2C=O)]$^+$[B(C_6F_5)$_4$]$^-$ had formed quantitatively. One set of broad, averaged resonances for free and coordinated Et_2C=O and sharp resonances for free Et_2CH−OH were observed. This evidence is consistent with the complete displacement of Et_2CH−OH from the W center upon addition of Et_2C=O, indicating that Et_2C=O binding is favored over Et_2CH−OH coordination. If 3% of total W is used as the NMR detection limit for the remaining W(Et_2-

Table 2. Crystallographic Collection and Refinement Data

	CpW(CO)$_2$(IMes)H	CpMo(CO)$_2$(IMes)H·0.5 (C_7H_8)	[CpW(CO)$_2$(IMes)]$^+$[B(C_6F_5)$_4$]$^-$·0.5(C_7H_8)	[CpW(CO)$_2$(IMes)(Et_2CH−OH)]$^+$-[B(C_6F_5)$_4$]$^-$
formula	$C_{28}H_{30}WN_2O_2$	$C_{31.5}H_{34}MoN_2O_2$	$C_{55.5}H_{33}BWF_{20}O_2$	$C_{57}H_{41}BWF_{20}O_3N_2$
fw	610.39	568.55	1334.50	1376.58
temp	293(2) K	293(2) K	150(2) K	150(2) K
cryst syst	triclinic	triclinic	monoclinic	orthorhombic
space group	$P\bar{1}$ (No. 2)	$P\bar{1}$ (No. 2)	$P2_1/c$ (No. 14)	*Pbca* (No. 61)
a (Å)	8.9340(18)	8.5080(17)	18.262(4)	17.636(4)
b (Å)	11.258(2)	16.515(3)	17.725(4)	17.126(3)
c (Å)	13.631(3)	21.351(4)	17.657(4)	35.532(7)
α (deg)	80.97(3)	106.97(3)		
β (deg)	72.96(3)	95.45(3)	113.87(3)	
γ (deg)	70.79(3)	92.94(3)		
V (Å^3)	1235.0(4)	2846.6(10)	5226.6(18)	5440
Z	2	4	4	8
μ (mm^{-1})	4.704	0.490	2.327	2.27
λ (Å)	0.71073	0.71073	0.90350	0.92200
ρ_{calc} (g cm^{-3})	1.641	1.327	1.696	1.704
cryst size (mm)	.33 × 0.33 × 0.27	0.60 × 0.40 × 0.25	.100 × 0.050 × 0.010	.050 × 0.050 × 0.005
θ range (deg)	2.40 to 27.47	2.01 to 26.00	3.02 to 28.25	1.49 to 31.16
total no. of reflns	5652	10 795	4800	22 257
no. of indep reflns, $I \geq 3.0\sigma(I)$	5652	10 795	4800	6833 [*R*(int) = 0.0693]
no. of params	299	660	749	758
final *R* indices [$I > 2\sigma(I)$]	R1 = 0.0284, wR2 = 0.0656	R1 = 0.0559, wR2 = 0.1206	R1 = 0.0573, wR2 = 0.1528	R1 = 0.0607, wR2 = 0.1539
R indices (all data)	R1 = 0.0681, wR2 = 0.0724	R1 = 0.2577, wR2 = 0.1596	R1 = 0.0585, wR2 = 0.1540	R1 = 0.0952, wR2 = 0.1733
goodness-of-fit on F^2	1.056	O.979	1.022	1.047
extinction coeff	none	none	none	none
absorp corr	ψ scans	Fourier(XABS2)[a]	none	Fourier(XABS2)[b]

[a] R1 = $\sum||F_o| - |F_c||/\sum|F_o|$; wR2 = $\{\sum[w(|F_o^2| - |F_c^2|)^2]/\sum[w|F_o^2|^2]\}^{1/2}$. [b] Parkin, S.; Moezzi, B.; Hope, H. *J. Appl. Crystallogr.* **1995**, *28*, 53−56.

$CH-OH)^+$ adduct, the lower limit of K_{eq} is estimated as $[W(Et_2C{=}O)^+][Et_2CH-OH]/[W(Et_2CH-OH)^+][Et_2C{=}O] > 100$.

Similarly, H_2 completely displaces coordinated $Et_2C{=}O$ from the $CpW(CO)_2(IMes)(Et_2C{=}O)^+$ adduct to yield the $CpW(CO)_2(IMes)(H)_2^+$ complex in C_6D_6. Moreover, $CpW(CO)_2(IMes)(H)_2^+$ remains intact upon addition of excess $Et_2C{=}O$ in C_6D_6. Additionally, introduction of H_2 to $CpW(CO)_2(IMes)(Et_2CH-OH)^+$ affords free Et_2CH-OH and $Cp_2W(CO)_2(IMes)(H)_2^+$ in C_6D_6, indicative of a stronger binding strength of H_2 versus Et_2CH-OH.

Example of Catalytic Hydrogenation at 54.4 atm (800 psi). $CpW(CO)_2(IMes)^+B(C_6F_5)_4^-$ (53.0 mg, 0.040 mmol) and 3-pentanone (1.20 mL, 11.3 mmol) were placed in a stainless steel high-pressure autoclave. H_2 (54.4 atm) was added, and the reaction was carried out in a constant-temperature bath. Prior to removal of each sample for analysis, the bottom of the autoclave was cooled at −196 °C, and the pressure was slowly vented. The autoclave was taken into a glovebox, and the sample for NMR analysis was removed. Then the autoclave was resealed and H_2 was again added.

Example of Catalytic Hydrogenation at 4 atm. $CpW(CO)_2(IMes)^+B(C_6F_5)_4^-$ (26.5 mg, 0.019 mmol) and 3-pentanone (600 μL, 5.65 mmol) were placed in a glass tube (125 mL capacity) equipped with a Teflon valve. The solution was freeze−pump−thawed, then frozen again, and the entire tube was submersed in liquid nitrogen. The tube was then filled with about 1 atm of H_2 at −196 °C, sealed, and warmed to room temperature. As a result, the tube contained 20 mmol of H_2 (ca. 4 atm at room temperature; $P_1/T_1 = P_2/T_2$, so when $P_1 = 1$ atm, $T_1 = 77$ K, $T_2 = 295$ K, the H_2 pressure in the sealed tube at 23 °C was ca. 4 atm). The reaction was carried out in a constant-temperature bath. Aliquots were removed by cooling the tube to −196 °C, evacuating the H_2, refilling the tube with Ar, and taking it into the glovebox. After removal of an aliquot (ca. 60 μL), the tube was again freeze−pump−thawed, filled with H_2 at −196 °C, and resealed.

X-ray Structure Determinations. X-ray crystallographic data sets for $CpW(CO)_2(IMes)H$ and $CpMo(CO)_2(IMes)H$ were collected on an Enraf Nonius CAD-4 diffractometer. The structures of **W** and **W(Et$_2$CHOH)** were determined from data collected at beamline X7B at the X-ray radiation at the National Synchrotron Light Source. Crystal data and information about the data collection are provided in Table 2.

Acknowledgment. Research at Brookhaven National Laboratory was carried out under contract DE-AC02-98CH10886 with the U.S. Department of Energy and was supported by its Division of Chemical Sciences, Office of Basic Energy Sciences. Research at Pacific Northwest National Laboratory was funded by the Division of Chemical Sciences, Office of Basic Energy Sciences, U.S. Department of Energy, and by an LDRD grant. Pacific Northwest National Laboratory is operated by Battelle for the U.S. Department of Energy.

Supporting Information Available: Additional ORTEPs of **W** and crystallographic information for **Mo**. This material is available free of charge via the Internet at http://pubs.acs.org.

OM700694E